NUREG/CR-4252
BNL-NUREG-51886

INDEPENDENT ASSESSMENT OF TRAC-PD2/MOD1 CODE WITH BCL ECC BYPASS TEST

G.C. Slovik and P. Saha

Date Published — April 1985

DEPARTMENT OF NUCLEAR ENERGY, BROOKHAVEN NATIONAL LABORATORY
UPTON, LONG ISLAND, NEW YORK 11973

Prepared for
U.S. Nuclear Regulatory Commission
Washington, D.C. 20555

NUREG/CR-4252
BNL-NUREG-51886
AN, R-4

INDEPENDENT ASSESSMENT OF TRAC-PD2/MOD1 CODE WITH BCL ECC BYPASS TESTS

G.C. Slovik and P. Saha

Manuscript Completed — March 1985
Date Published — April 1985

LWR CODE ASSESSMENT AND APPLICATION GROUP
DEPARTMENT OF NUCLEAR ENERGY
BROOKHAVEN NATIONAL LABORATORY
UPTON, LONG ISLAND, NEW YORK 11973

PREPARED FOR
UNITED STATES NUCLEAR REGULATORY COMMISSION
OFFICE OF NUCLEAR REGULATORY RESEARCH
WASHINGTON, D.C. 20555
CONTRACT NO. DE-AC02-76CH00016
NRC FIN-3257

TABLE OF CONTENTS

LIST OF TABLES

LIST OF FIGURES

List of Figure (cont)

List of Figure (cont)

List of Figure (cont)

ABSTRACT

This report presents the TRAC-PD2/MOD1 independent assessment calculations performed at Brookhaven National Laboratory (BNL) using the Emergency Core Cooling (ECC) bypass experiments conducted in a 2/15-scale PWR vessel at Battelle Columbus Laboratories (BCL). Both steady-state experiments with various ECC water subcoolings and transient tests with hot wall effects were simulated. Besides the base cases, several sensitivity calculations were performed to study the effects of nodalization, particularly the relative locations of the hot leg penetrations in the downcomer. In addition, calculations were performed to determine the effect of slight increases in the reverse core steam flow and the associated form losses due to the hot leg penetrations. Code corrections as received from the code developers at Los Alamos National Laboratory (LANL) were also incorporated during this study.

The TRAC-PD2/MOD1 code results were found to be highly sensitive to nodalization and other input parameters. Thus, good agreement with the experimental data could be fortuitous. However, the code does calculate a strong multidimensional flow behavior in a PWR downcomer during the refill period, and has the potential to be a very useful tool for best-estimate or realistic analysis of PWR large break LOCA.

EXECUTIVE SUMMARY

The TRAC-PD2/MOD1 code, which is an updated version of the TRAC-PD2 code developed at Los Alamos National Laboratory (LANL), has been assessed at Brookhaven National Laboratory (BNL) using the ECC (Emergency Core Cooling) bypass experiments conducted at Battelle Columbus Laboratories (BCL). As a best-estimate PWR LOCA code, TRAC-PD2/MOD1 is expected to accurately predict all three major stages, namely, the blowdown, refill, and reflood, of a large-break LOCA in a PWR.

The objective of the present study is to assess the capability of TRAC-PD2/MOD1 in predicting the refill stage, i.e., the lower plenum filling rate after the ECC water is injected into the cold legs of a PWR system. The ECC water penetration rate (or the lower plenum filling rate) depends on the water injection rate, water temperature (or subcooling), reverse core steam flow rate, system pressure, and equipment size or scale. Moreover, the process of water penetration is the result of many interacting phenomena such as countercurrent flow limitation (CCFL), direct-contact condensation, steam generation due to hot walls, and asymmetric (multi-dimensional) flow behavior. Thus, an accurate prediction of the ECC-bypass test is a formidable task for any code.

A large number of steady-state and transient ECC-bypass experiments in a 2/15-scale PWR vessel were conducted at BCL. Two series of steady-state tests and one transient test were chosen for simulation with the TRAC-PD2/MOD1 code at BNL:

(i) Test IDs = 26715 and 26719 (steady-state tests with "low" subcooling)

(ii) Test IDs = 26502 and 26505 (steady-state tests with "high" subcooling)

(iii) Test ID = 29302 (a transient test with "hot" wall).

Besides the base cases, several sensitivity calculations were performed to study the effects of nodalization, particularly the relative locations of the hot leg penetrations in the downcomer. In addition, calculations were performed to determine the effect of slight increases in the reverse core steam flow and the associated form losses due to the hot leg penetrations. Corrections as received from the code developers at LANL were also incorporated in the code.

The major conclusions from the study are the following:

1. The TRAC-PD2/MOD1 code may predict the ECC bypass (or ECC delivery into the lower plenum) during a PWR large-break LOCA with reasonable success. However, the code results are highly sensitive to nodalization and the relative locations of the hot leg penetrations in the downcomer annulus. This precludes making any firm statement about the code accuracy and providing user guidelines for PWR LOCA studies.

2. The code does calculate a strong multidimensional flow behavior expected in a PWR downcomer during the refill stage of a large break LOCA. Thus, the code has the potential to be a very useful tool for best-estimate or realistic analysis of PWR large break LOCA.

It is recommended that the code developers at LANL reexamine the code very carefully for possible coding errors. The constitutive package should be scrutinized again because some of the correlations as used in the code are node-size dependent. Also, various nodalizations, particularly various relative locations of the hot leg penetrations, should be attempted while applying the TRAC-PD2/MOD1 code to the PWR large-break LOCA analysis in order to investigate their effects on the predicted peak clad temperature (PCT).

ACKNOWLEDGMENTS

The authors would like to thank Drs. F. Odar and N. Zuber of USNRC for their suggestions and comments during this study. Special thanks are due L. J. Flanigan and R. P. Collier of BCL for providing additional information on the ECC-bypass experiments, and D. R. Liles, T. D. Knight, and J. Meier of LANL for many helpful discussions and code corrections. Finally, the fine typing by Ms. Ann C. Fort and editing by Ms. Mary Rustad are highly appreciated.

1. INTRODUCTION

1.1 Background

TRAC-PD2/MOD1 is an updated version of TRAC-PD2 code (Liles, 1981a) which is a best-estimate advanced systems code for analysis of Loss-of-Coolant Accident (LOCA) in Pressurized Water Reactors (PWRs). The code was developed at Los Alamos National Laboratory (LANL) under the sponsorship of the U.S. Nuclear Regulatory Commission (USNRC).

Extensive assessment or verification of TRAC-PD2 and TRAC-PD2/MOD1 has been performed at three different national laboratories, namely, Brookhaven National Laboratory (BNL), Idaho National Engineering Laboratory (INEL), and, of course, LANL. All TRAC-PD2 assessment efforts conducted at BNL were presented in an earlier report (Saha, 1982a). This report will present the TRAC-PD2/MOD1 assessment work performed at BNL using the Battelle Columbus Laboratory (BCL) ECC-Bypass experiments (Segev, 1980).

It is known that a large-break LOCA in a PWR occurs in three distinct stages: (a) blowdown, (b) refill, and (c) reflood. Each of these stages is governed by different dominant phenomena and influences the peak cladding temperature. Thus, a LOCA code such as TRAC-PD2 or TRAC-PD2/MOD1 should be assessed with separate-effects tests pertinent to each of these stages. BNL assessment of TRAC-PD2 with separate-effect blowdown tests (e.g., Moby-Dick, BNL nozzle, Super-CANON, Marviken) and reflood tests such as FLECHT-SEASET experiments has been reported earlier (Saha, 1982a). TRAC-PD2 assessment with the refill tests, e.g., BCL ECC-bypass experiment, was also initiated at BNL in FY 1981. However, several updates and corrections to the TRAC-PD2 code were received at BNL from LANL before this task was completed. Therefore, the BCL experiments were analyzed a second time using the updated code, i.e., TRAC-PD2/MOD1. This report will present those results and discuss the areas where the code needs further improvements, particularly for the refill stage of a PWR LOCA.

1.2 Objective

The objective of the present study is to assess the capability of TRAC-PD2/MOD1 in predicting the lower plenum filling rate after the Emergency Core Cooling (ECC) water is injected during a postulated large-break LOCA in a PWR system. The ECC water penetration rate (or the lower plenum filling rate) depends on the water injection rate, water temperature (or subcooling), reverse core steam flow rate, system pressure, and equipment size or scale. Moreover, the process of water penetration is the result of many interacting phenomena such as countercurrent flow limitation (CCFL), direct-contact condensation, and steam generation due to hot walls and asymmetric (multidimensional) flow behavior. Thus, an accurate prediction of the ECC-bypass test is a formidable task for any code.

The BCL staff had conducted several steady-state and transient ECC-bypass experiments in a 2/15-scale PWR vessel (Segev, 1980). Two series of steady-state tests and one transient test were chosen for simulation with the TRAC-PD2/MOD1 code at BNL:

(i) Test ID = 26715 - 19 (steady-state tests with "low" subcooling)
(ii) Test ID = 26502 - 07 (steady-state tests with "high" subcooling)
(iii) Test ID = 29302 (a transient test with "hot" wall).

Besides assessing the thermal-hydraulic models, we have also studied the sensitivity of code results to various nodalizations including the relative positions of the hot leg plugs (or penetrations) in the test vessel. This was performed in order to provide guidance to the TRAC-PD2 and TRAC-PD2/MOD1 code users.

1.3 Brief Description of TRAC-PD2/MOD1

As mentioned earlier, the TRAC-PD2/MOD1 code (Version 27.0) was generated by updating the TRAC-PD2 code (Liles, 1981a). Specific updates that were used are given in TRAC NEWS No. 5 (Harper, 1981). These updates were

developed to correct FORTRAN or coding error, but not to change the physical models used in TRAC-PD2. Therefore, the physical models of TRAC-PD2 and TRAC-PD2/MOD1 are essentially the same.

Detailed description of the TRAC-PD2 code can be found in Liles (1981a). However, a brief description of this code may help to better understand the assessment calculations that follow this introduction.

The code consists of several modules, namely, VESSEL, PIPE, TEE, PRESSURIZER, STEAM GENERATOR, PUMP, VALVE, etc., to represent the various components of a PWR system. By suitably connecting these modules, one may model a reactor system or a wide spectrum of integral as well as separate-effects test facilities. Two special components, namely, BREAK and FILL, are used to provide the boundary conditions. In addition, models for structural heat transfer and point-reactor kinetics are also included in the code.

The VESSEL module represents the reactor vessel of a PWR. By suitable partitioning and nodalization, one can model the upper and lower plena, the downcomer, and the core within this module. The thermal-hydraulics of this module is based on a six-equation, two-fluid, three-dimensional formulation of two-phase flow. Conservation of mass and energy for the two-phase mixture and the vapor phase is employed. Also, two phasic equations of motion, one for the liquid and the other for the vapor, are used. These two equations are then resolved into three coordinates, namely, the axial, radial, and azimuthal, to calculate the phasic velocities in three directions. In addition, constitutive relations for the interfacial and wall-to-fluid momentum and heat transfer are needed and used to close the formulation. These constitutive relations play a major role in the code predictions, and the assessment activities at BNL are directed at verifying their adequacy or reliability in various situations pertinent to the LWR safety.

All the other TRAC-PD2 modules are based on a one-dimensional, five-equation, drift-flux formulation of two-phase flow. Like the VESSEL module, these components also use the conservation of mass and energy for the mixture and the vapor phase. However, they use only one equation of motion for the center of mass of the mixture. Therefore, a constitutive relation for the relative velocity between the phases is specified to determine the two phasic velocities. Furthermore, as in the two-fluid model, constitutive relations for the interfacial heat and mass transfer and the wall-to-fluid heat and momentum transfer are added to close the formulation. It should be stressed that all the components of TRAC are based on nonhomogeneous and nonequilibrium formulation of two-phase flow. In addition, since TRAC uses two energy equations, it does not restrict either liquid or vapor phase at saturation.

The partial differential equations that describe the TRAC-PD2 two-phase flow and heat transfer models are solved by finite differences. The heat transfer equations are treated using a semi-implicit differencing technique, whereas the hydrodynamic equations are treated using either a semi-implicit or fully implicit differencing under user control. The resultant system of coupled, nonlinear, algebraic equations is then solved by a Newton-Raphson iteration procedure.

1.4 Report Outline

The BCL test facility, test procedure, and test results of the selected experiments are described in Chapter 2. This is followed by the TRAC-PD2/MOD1 input model description. In Chapter 4, the results of the TRAC base calculations are compared with the experimental data, and some observations are made. Further code calculations or sensitivity studies along with some discussions are presented in Chapter 5. Finally, the conclusions and recommendations are presented in Chapter 6.

2. TEST DESCRIPTION

2.1 Test Facility and Instrumentation

Battelle Columbus Laboratories (BCL) ran several Emergency Core Cooling (ECC) bypass tests in their 2/15th-scale model of a typical pressurized water reactor vessel to assist in the advanced code assessment (Segev, 1980). The test facility consisted of a pressure vessel 2.5 m tall with an inside diameter of 0.62 m. There was a steam feed line at the top of the upper plenum and a lower plenum drain line located at the bottom of the vessel. The downcomer gap width was 0.0312 m with an adjacent core barrel 1.1 m long. Both the pressure vessel and the core barrel walls were thick so as to provide a hot wall capability to simulate the additional steam generation during an ECC bypass transient. The two hot legs were simulated by plugs of 0.2 m diameter in the downcomer annulus, while the four cold legs of 0.102 m inside diameter were pipe construction with a 60^{o}-120^{o} orientation. The model as built is shown in Figure 2.1.

The experimental measurements included the volumetric flow rate and temperature of water and steam entering the test vessel along with the steam supply pressure. The wall and fluid temperatures as well as the differential pressures at various locations in the downcomer were also monitored. In addition, a number of three-prong detectors were used to indicate the presence of steam or water throughout the annulus. The lower plenum measurement included the water level (by a conductivity probe), fluid temperatures, and absolute pressure. The fluid density, temperature, momentum flux, and pressures were measured in the broken leg. In the containment, i.e., at the exit of the broken cold leg, pressure, temperature, and water level were measured. However, in the data report (Segev, 1980), only a limited number of measured quantities were reported.

The measurement accuracies are reported in Appendix A of (Cudnik, 1978). The expected errors in the most pertinent measurements are as follows:

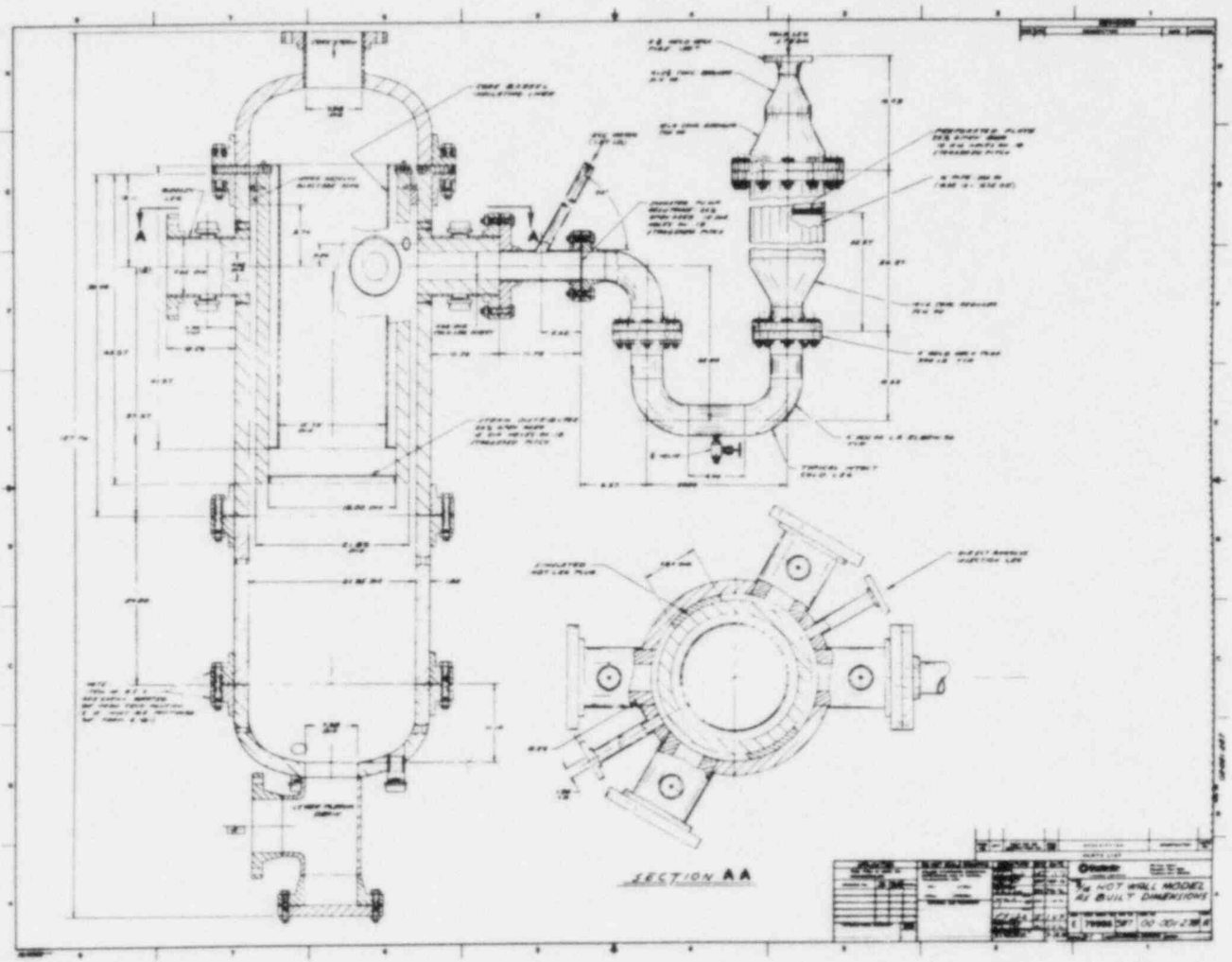

Figure 2.1 BCL ECC-Bypass Test Facility. (BNL Neg. No. 1-38-85)

a) Lower plenum pressure = ± 0.5 psia (3.45 kPa)
b) Lower plenum water level = ± 1 in (0.0254 m)
c) Wall surface and fluid temp. = ± 2 °F (1.1°C)
d) Water and steam flow rate = ± 0.5%

The details of the test facility and instrumentation can be found in a BCL topical report (Cudnik, 1978).

2.2 Tests Selected for TRAC Assessment

BCL performed two types of tests. The first type was the steady-state plenum filling experiment. These experiments were performed by setting the pressures, temperatures, and flow rates (for both steam and ECC water) at the desired conditions with the lower plenum drain open and the plenum liquid level under automatic control. When steady conditions were reached, the liquid level was lowered and the drain valve was closed. The plenum was then allowed to fill, and the water delivery rate into the lower plenum was determined from the water level measurement. By varying the steam flow rate, a steady counter-current flow limitation (CCFL) curve for the same ECC water flow rate was generated.

The second type of experiment consisted of transient tests with steam rampdown to simulate the changing core steam flow rate during the refill stage of a LOCA. In some of these experiments, the initial vessel wall temperature was higher than the steam temperature to simulate additional vapor generation due to hot wall effects during a LOCA. The vessel wall was heated to the desired temperature by blowing hot air inside and outside the vessel (Flanigan, 1983). Steam flow was initiated to purge the air from inside the vessel, and the system was allowed to reach a steady state. The transient was initiated by simultaneously injecting the ECC water and ramping the steam flow rate down.

In the BNL assessment effort, both types of experiments were simulated using the TRAC-PD2/MOD1 code. For the steady state tests, two series of experiments were chosen, namely, Test IDs = 26715 - 19 and 26502 - 07. However, because of time and resource limitations, only the end points of these test series were simulated. The nominal operating conditions of the tests simulated are shown in Table 2.1. Notice that the Test IDs = 26716 and 26719 represent a "low" subcooling situation, whereas the Test IDs = 26502 and 26505 are typical of "high" subcooling situations expected during the refill stage of a LOCA. Simulation of these two highly different subcooling tests would also help assess the direct contact condensation models used in TRAC-PD2/MOD1.

From the transient tests, Test ID = 29302 with hot walls was selected for simulation. The nominal conditions of this test are shown in Table 2.2, and the histories of several important parameters, as measured, are shown in Figure 2.2. ECC water injection was started at approximately 11.5 s, and the containment pressure was almost constant at 2.08 bar.

Table 2.1 Nominal Conditions of the Steady State Tests

Test ID	Core Steam Flow Rate (kg/s)	Total ECC Water Inj. Rate (kg/s)	Water Penetra. Rate (kg/s)	ECC Water Subcooling* (°C)	Lower Plenum Pressure (bar)	Containment Pressure + (bar)
26716	1.201	23.038	6.018	29.9	2.6662	0.9956
26719	0.877	23.020	11.437	26.3	2.3028	1.8037
26502	1.639	15.803	14.049	95.6	2.1912	2.1002
26505	2.037	15.858	0.649	93.5	2.0582	1.4859

* Based on Lower Plenum Saturation Temperature
+ Obtained through Private Communications (Collier, 1981; Flanigan, 1982)

Table 2.2 Nominal Conditions of the Transient Test

Test ID	Average Lower Plenum Pressure (bar)	Initial Lower Plenum Pressure (bar)	Initial Vessel Wall Temp (°C)	Initial Steam Flow Rate (kg/s)	Water Inj. Rate (kg/s)	Injected Water Temperature (°C)
29302	3.585	2.899	273.9	1.714	22.52	100.0

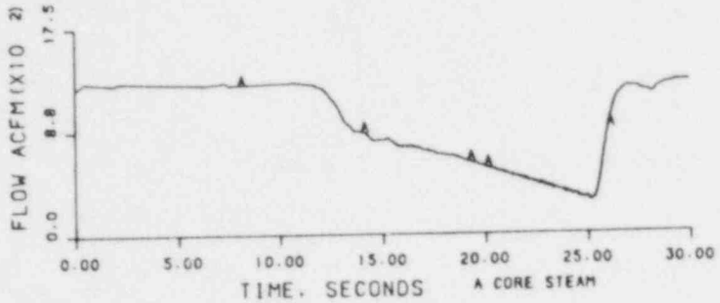

(a)

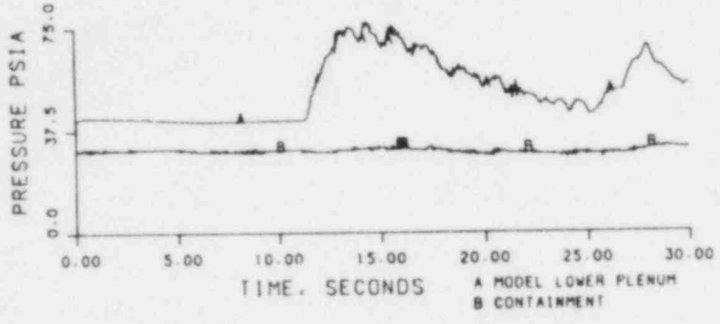

(b)

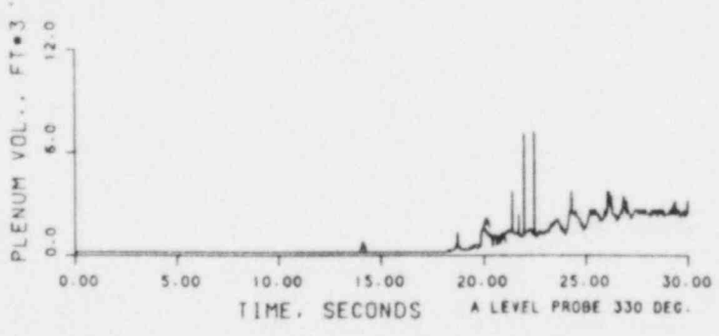

(c)

Figure 2.2 Variation of (a) Core Steam Flow Rate, (b) Model Lower Plenum and Containment Pressure, and (c) Lower Plenum Liquid Volume vs. Time for BCL Test 29302. (BNL Neg. No. 1-39-85)

3. TRAC INPUT MODEL DESCRIPTION

The BCL test facility was modeled by using several TRAC components. The test vessel was modeled with the VESSEL module of TRAC with two radial rings and nine axial levels. The inner radial ring represented the core barrel, whereas the outer ring represented the downcomer annulus. In the axial direction, the bottom three levels represented the lower plenum, and the upper six levels modeled the downcomer and core barrel regions. During preliminary calculations six azimuthal sectors were used, as it seemed logical to centrally position all six pipe connections (four cold legs and two hot leg plugs) into the vessel. However, the computer running time for this model with 108 cells in the VESSEL module was prohibitively high (e.g., the CPU-to-real time ratio of ~700 in the BNL CDC-7600 computer). Therefore, in accordance with the suggestions of the code developers (Liles, 1981b), four 90° azimuthal sectors were used in all subsequent runs.

The new nodalization with 72 cells in the VESSEL module is shown in Figure 3.1. This reduction in the number of vessel cells (< 80) enabled us to use the direct matrix inversion method for vessel equations which significantly reduced the computer running time (by about a factor of 4). However, there was also a question of how to model the hot leg plugs in the new nodalization. This is explained by Figure 3.2 where the downcomer annulus has been unwrapped. Several choices exist. One could place the azimuthal cell boundaries such that both hot leg plugs would completely reside inside the cells as shown by the vertical solid lines (1) in Figure 3.2. The presence of hot leg plugs, in this case, is modeled by reducing the appropriate cell volumes, but not the azimuthal flow areas. Or one may shift the azimuthal cell boundaries slightly so that the hot leg plugs would reside on the cell boundaries as shown by the vertical dashed lines (2) in Figure 3.2. In this case, the hot leg plugs would reduce <u>both</u> the cell effective volumes and the azimuthal flow areas. Another choice is, of course, to ignore the effects of hot leg plugs altogether. This has been the practice at LANL (Meier, 1981). In the present assessment effort, all the above three choices were considered and three calculations have been performed

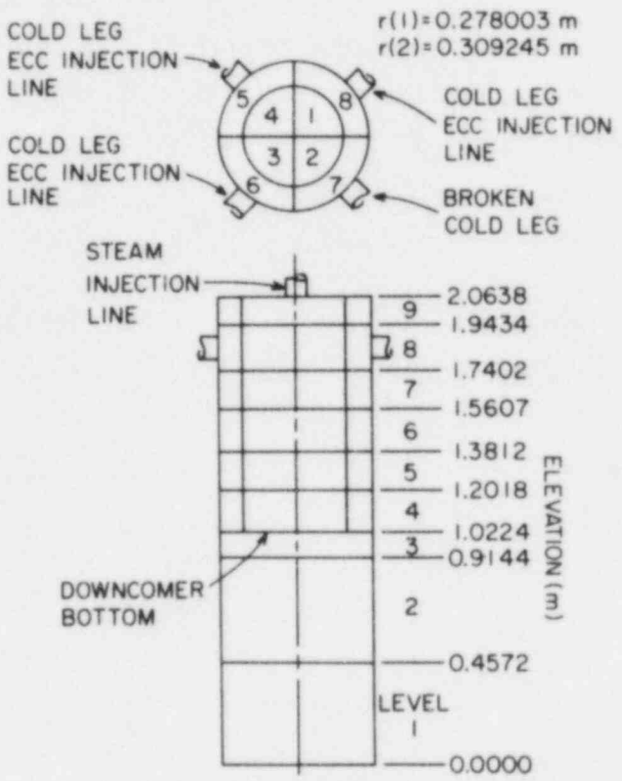

Figure 3.1 Vessel Nodalization for TRAC Input Model.
(BNL Neg. No. 10-941-81)

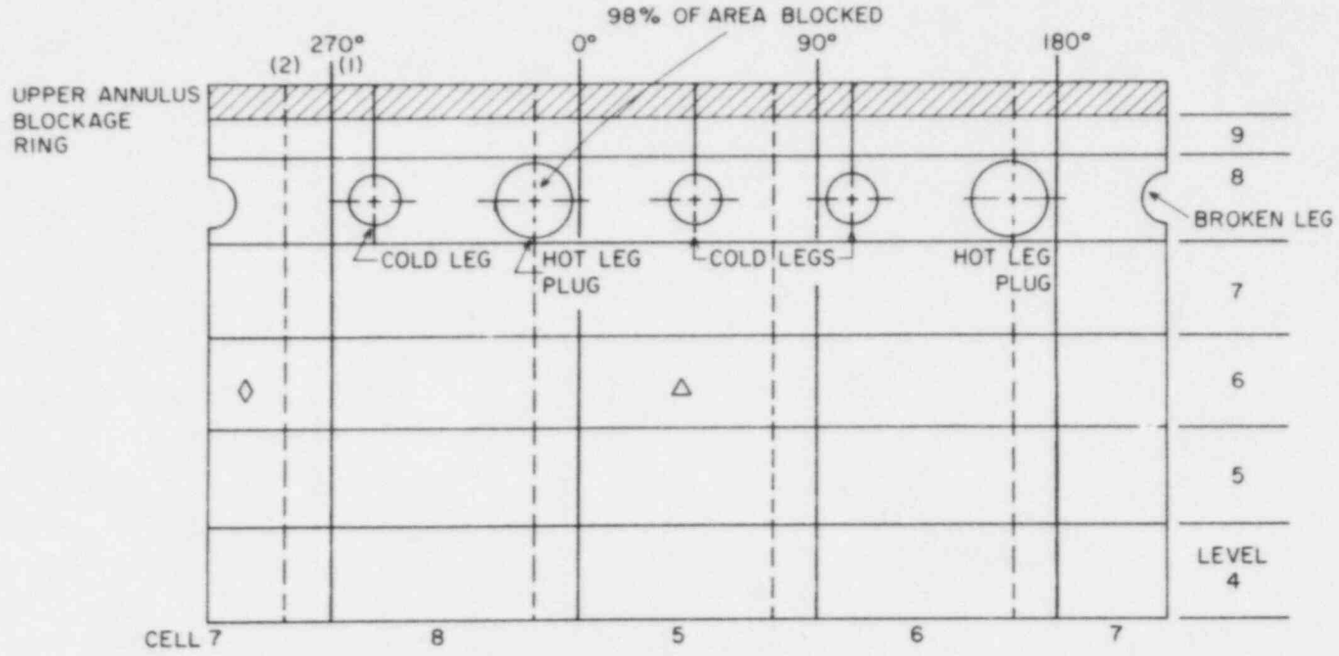

(1) NODING FOR THE HOT LEG PLUGS INSIDE THE CELL
(2) NODING FOR THE HOT LEG PLUG ON THE BOUNDARY OF THE CELL

△ ANNULUS FLUID TEMPERATURE
◊ PRESSURE VESSEL INNER WALL TEMPERATURE

Figure 3.2 Location of Hot Leg Plugs Relative to Azimuthal Cell Boundaries. (BNL Neg. No. 1-40-85)

for the transient test ID = 29302. For the steady-state tests, however, a compromise between the two extreme nodalizations (0% and 98% blockage) was made for the base calculations. The azimuthal cell boundaries were placed such that the azimuthal flow areas in Level 8 would be reduced by 50%. The results of these calculations will be presented in Chapter 4.

The input model was completed by attaching four PIPE components at the top of the vessel to represent the steam feedline, and four PIPE components at Level 8 to represent the four cold legs including the broken one. The steam lines and the three intact cold legs were each 0.1 m long. FILL components were connected to the other end of these pipes to introduce the experimental flow rates of steam and ECC water as functions of time. The broken cold leg was 1.56 m long and divided into 7 cells. The other end of this broken leg was connected to a BREAK component where the experimental values of containment pressure were used as boundary conditions. Also, an additive loss coefficient (FRIC) was used in the first cell of the broken leg to represent the irreversible losses due to entrance effects, the drag disk and instrument rake placed in the broken leg. The value of this loss coefficient was obtained from the measured pressure drop across the broken leg prior to the transient tests when only steam was flowing. On the basis of the appropriate test data, an additive loss coefficient of 0.235 was used for Test IDs = 26502 to 26719, whereas a value of 0.5 was used for Test ID = 29302. (Changes in the instrument rake resulted in different values for the loss coefficient.) A listing of the input deck used for Test ID = 26716 is provided in the Appendix as an example.

Finally, the TRAC-PD2/MOD1 (Version 27.0) code with two BNL updates was used for all the base calculations to be presented in Chapter 4. These BNL updates (Saha, 1981) corrected some coding errors in the interfacial shear package in TF3DE subroutine of the TRAC VESSEL module.

4. CODE PREDICTION AND COMPARISON WITH DATA

4.1 Steady-State Experiments

As mentioned earlier, two series of steady-state experiments, i.e., one with "low" ECC water subcooling (Test IDs = 26716 and 26719) and the other with "high" ECC water subcooling (Test IDs = 26502 and 26505), were simulated. For all these runs, the azimuthal cell boundaries were placed such that the two hot leg plugs would block 50% of corresponding azimuthal flow areas in Level 8. The core steam flow rates, the ECC water flow rates, and the containment pressures were kept fixed at the appropriate experimental values as shown in Table 2.1, and the code was run for 15 to 30s of problem time. Important parameters such as break flow rates, lower plenum filling rates, and lower plenum pressures were monitored and compared with experimental data.

4.1.1 Low ECC Water Subcooling Tests

Figures 4.1 through 4.4 show the comparison between the measured and predicted values of break mass flow rate, fluid density in the broken leg, lower plenum water level, and the lower plenum pressure for Test ID = 26716. In this test, most of the water injected bypassed the lower plenum and went out through the break. The TRAC calculation also shows that trend. However, the predicted bypass or break flow rate is slightly higher (see Figure 4.1) which resulted in a slightly lower filling rate as shown in Figure 4.3. This lower filling rate is consistent with the somewhat higher lower plenum pressure (Figure 4.4) predicted by TRAC. In general, the TRAC-PD2/MOD1 prediction of Test ID = 26716 with the chosen noding is quite good.

Figures 4.5 through 4.8 show similar comparisons for Test ID = 26719. In this test, approximately 50% of the injected water is bypassed; on the average, TRAC also predicts the same behavior (see Figure 4.5). Thus the lower plenum filling rate and the lower plenum pressure are also well predicted by TRAC.

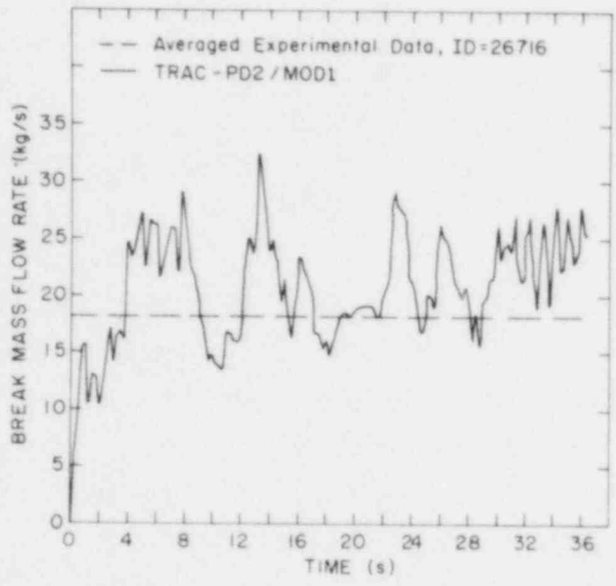

Figure 4.1 Comparison Between the TRAC-PD2/MOD1 Prediction and the Experimental Data for Break Mass Flow Rate for Test ID = 26716. (BNL Neg. No. 1-41-85)

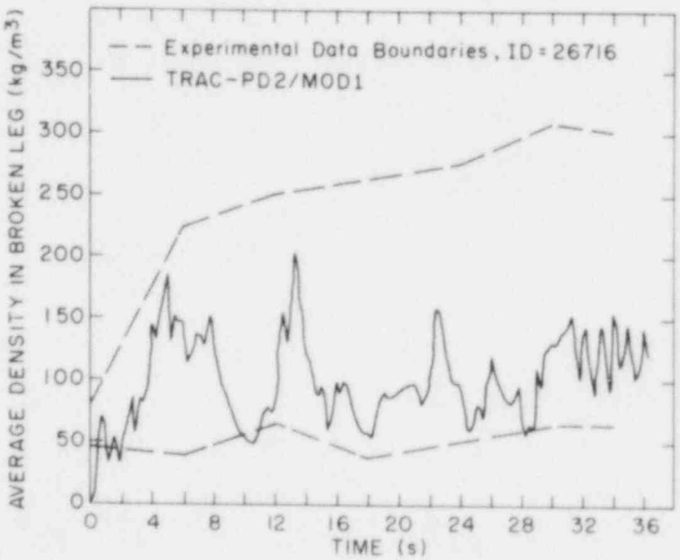

Figure 4.2 Comparison Between the TRAC-PD2/MOD1 Prediction and the Experimental Date for Average Fluid Density in Broken Leg for Test ID = 26716. (BNL Neg. No. 1-42-85)

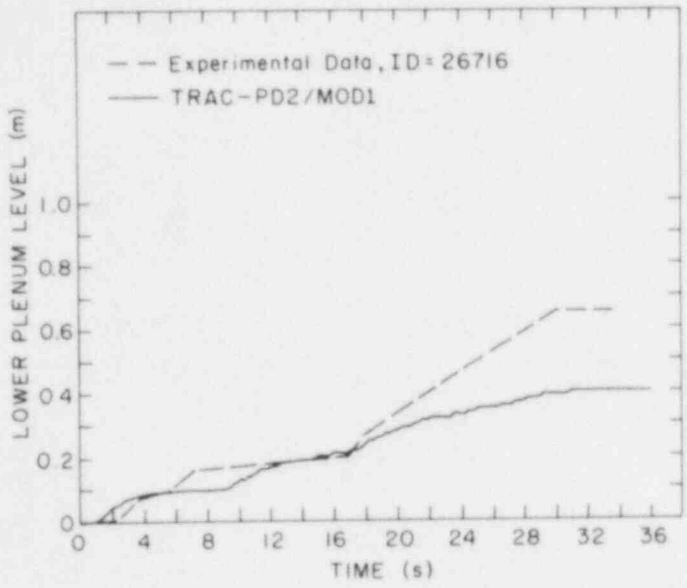

Figure 4.3 Comparison Between the TRAC-PD2/MOD1 Prediction and the Experimental Data for Lower Plenum Water Level for Test ID = 26716. (BNL Neg. No. 1-44-85)

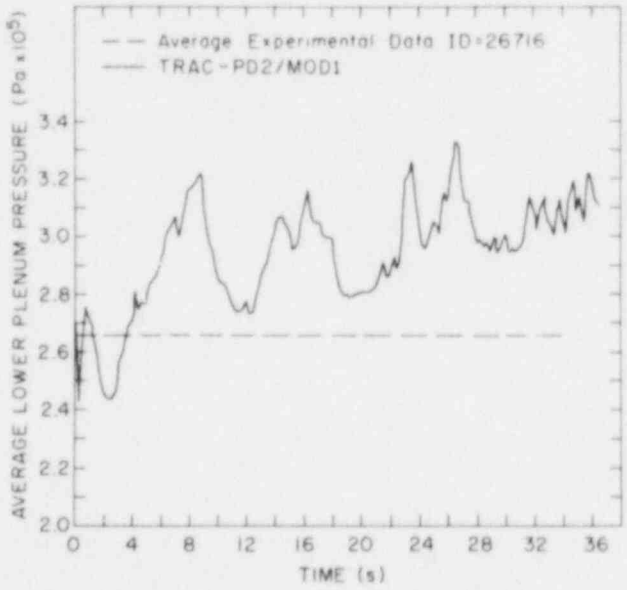

Figure 4.4 Comparison Between the TRAC-PD2/MOD1 Prediction and the Experimental Data for Lower Plenum Pressure for Test ID = 26716. (BNL Neg. No. 1-43-85)

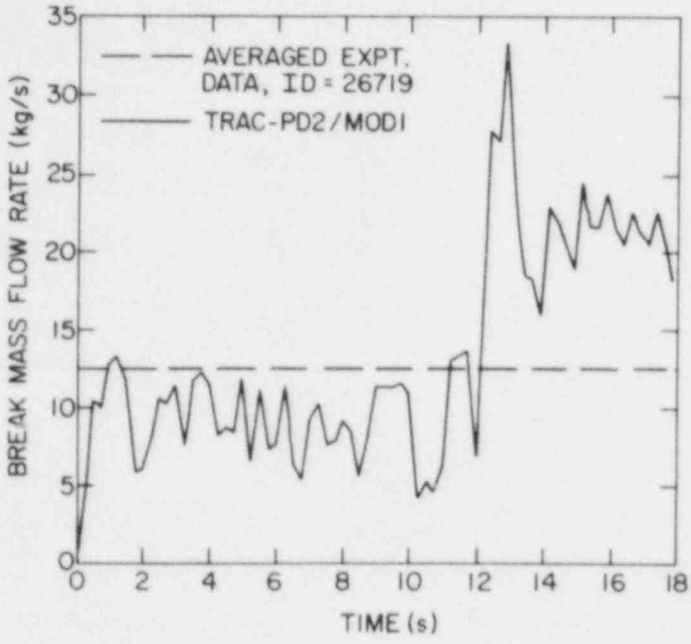

Figure 4.5 Comparison Between the TRAC-PD2/MOD1 Prediction and the Experimental Data for Break Mass Flow Rate for Test ID = 26719.(BNL Neg. No. 1-320-85)

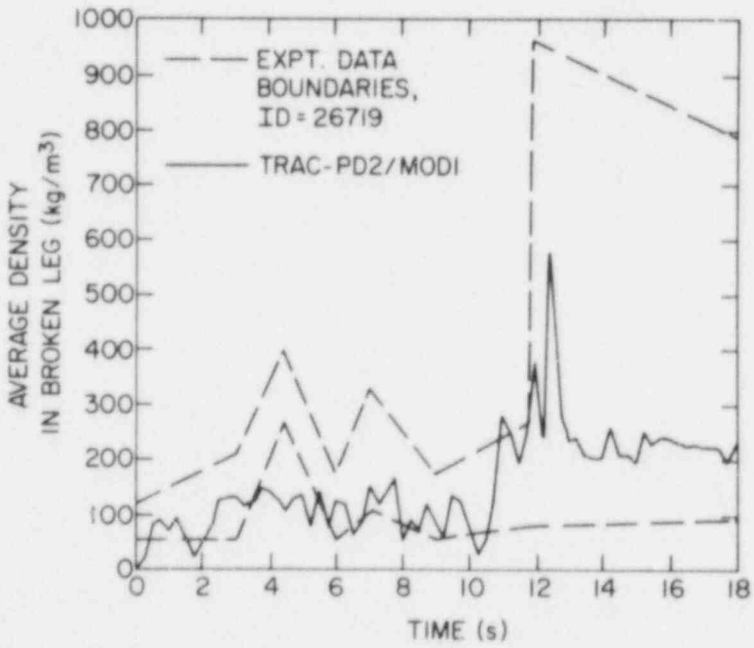

Figure 4.6 Comparison Between the TRAC-PD2/MOD1 Prediction and the Experimental Data for Average Fluid Density in Broken Leg for Test ID = 26719. (BNL Neg. No. 1-321-85)

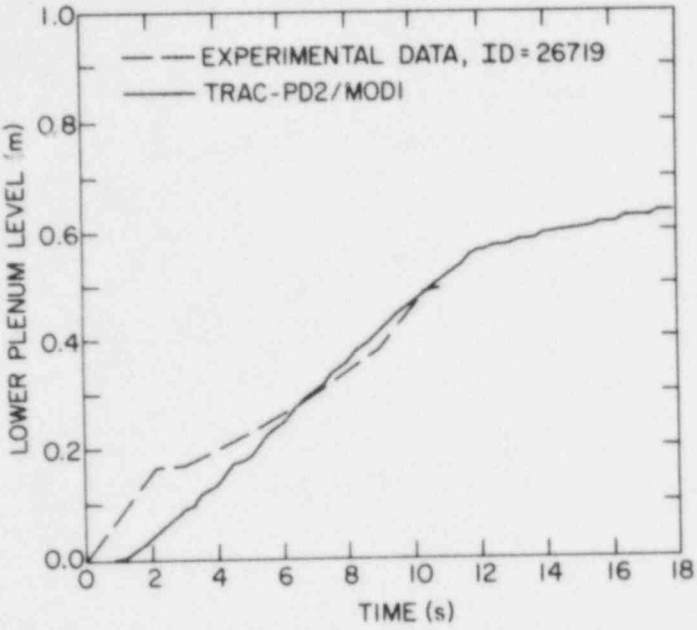

Figure 4.7 Comparison Between the TRAC-PD2/MOD1 Prediction and the Experimental Data for Lower Plenum Water Level for Test ID = 26719. (BNL Neg. No. 1-322-85)

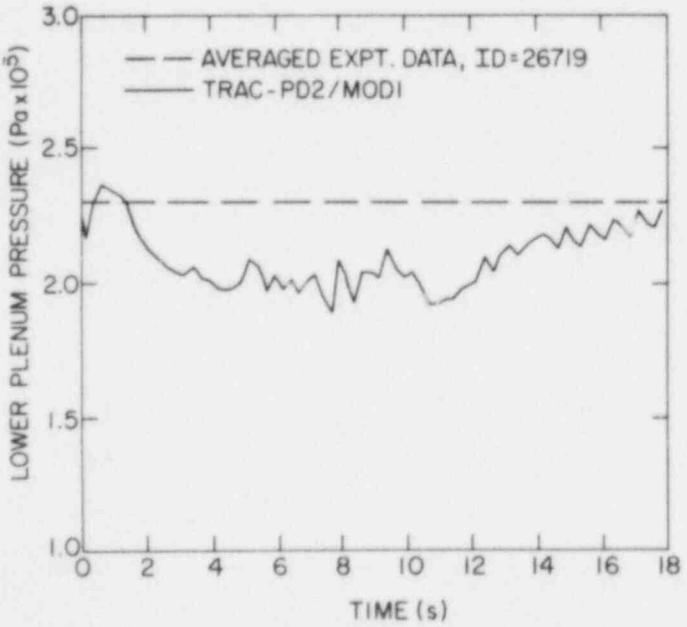

Figure 4.8 Comparison Between the TRAC-PD2/MOD1 Prediction and the Experimental Data for Lower Plenum Pressure for Test ID = 26719. (BNL Neg. No. 1-385-85)

Finally, Figure 4.9 shows the comparison of the average liquid penetration rate for Test IDs = 26716 and 26719. Reasonably good agreement between the test data and TRAC-PD2/MOD1 prediction has been obtained with the chosen nodalization. The effect of nodalization will be further discussed in Chapter 5.

4.1.2 High ECC Water Subcooling Tests

Figures 4.10 through 4.13 show the comparison between the measured and predicted values of break mass flow rate, fluid density in the broken leg, lower plenum water level, and lower plenum pressure for Test ID = 26502. As shown in Table 2.1, most of the ECC water injected was delivered into the lower plenum. TRAC also predicted this complete water delivery without a bypass situation as measured in the experiment. It can be seen from Figure 4.10 that virtually no water was predicted to be bypassed; on the contrary, steam from the containment was occasionally sucked into the pressure vessel. This was caused by a somewhat lower calculated pressure in the vessel as a result of steam condensation on highly subcooled ECC water. Therefore, the TRAC-predicted water delivery rate was slightly higher than that measured in the experiment.

The situation was completely different for Test ID = 26505. In this test, the reverse core steam flow was high enough to bypass most of the ECC injection. Thus, the water delivery rate into the lower plenum was very small. The comparisons between the measured and predicted values of the pertinent parameters for this test are shown in Figures 4.14 through 4.17. Unlike the three preceding calculations, TRAC did not correctly predict the experimental trend for this test. The code severely underpredicted the break flow rate (Figure 4.14) and overpredicted the lower plenum filling rate (Figure 4.16). However, this is consistent with the underprediction of lower plenum pressure as shown in Figure 4.17. It seems that overprediction of condensation rate caused the underprediction of pressure which, in turn, caused excessive water delivery into the lower plenum.

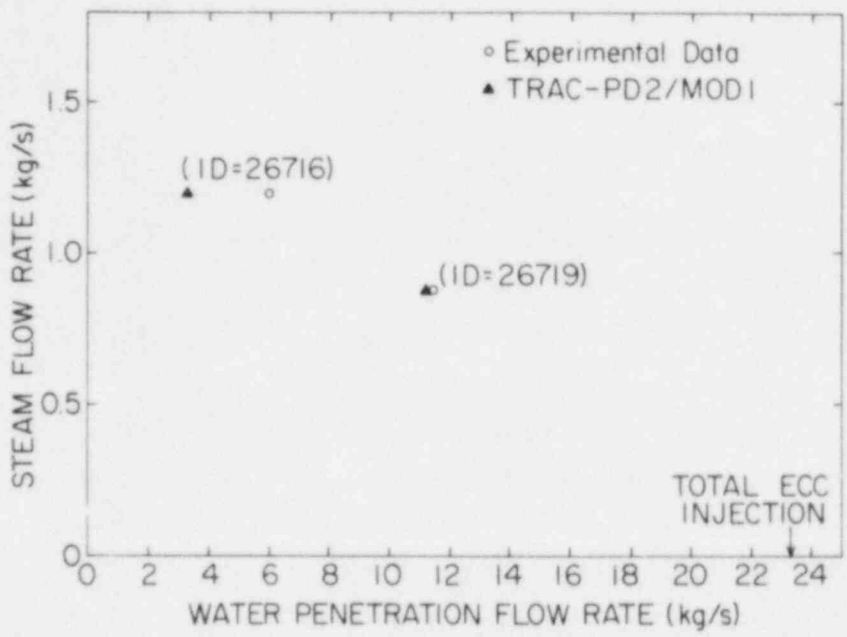

Figure 4.9 Comparison Between the TRAC-PD2/MOD1 Prediction and the Experimental Data for Average Water Penetration or Filling Rate for Test ID = 26716 and 26719. (BNL Neg. No. 1-383-85)

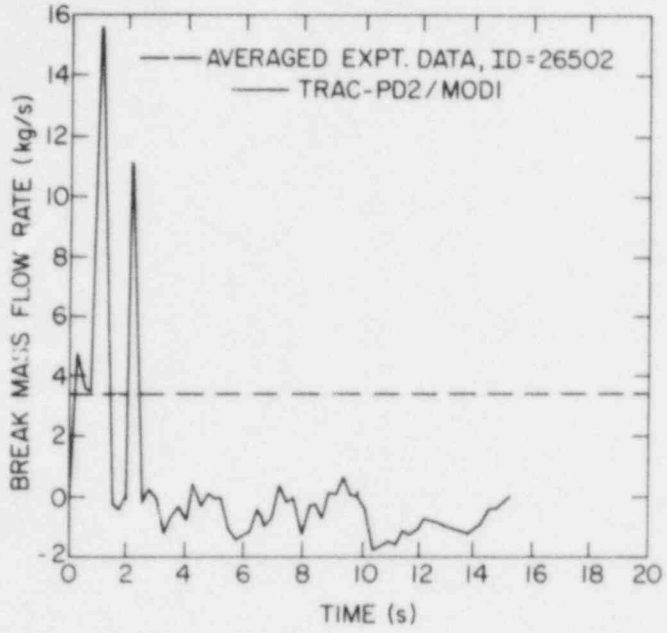

Figure 4.10 Comparison Between the TRAC-PD2/MOD1 Prediction and the Experimental Data for Break Mass Flow Rate for Test ID = 26502. (BNL Neg. No. 1-384-85)

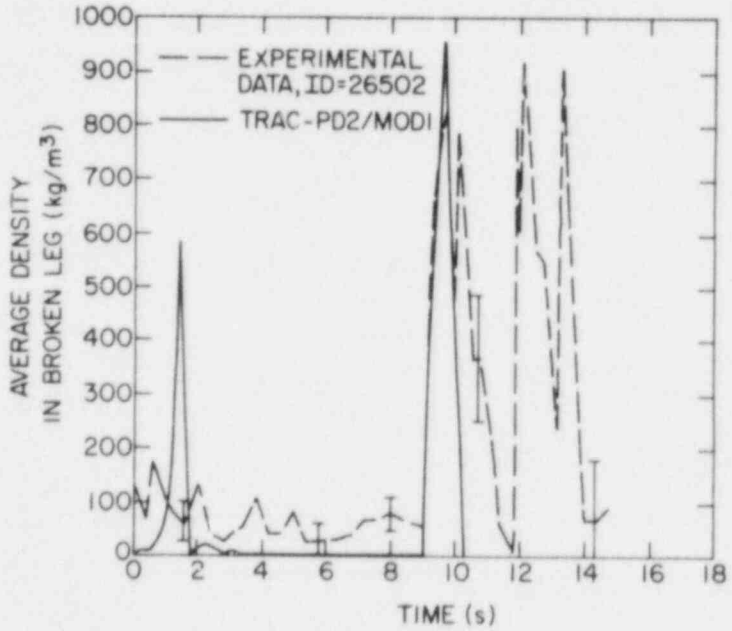

Figure 4.11 Comparison Between the TRAC-PD2/MOD1 Prediction and the Experimental Data for Average Fluid Density in Broken Leg for Test ID = 26502. (BNL Neg. No. 1-324-85)

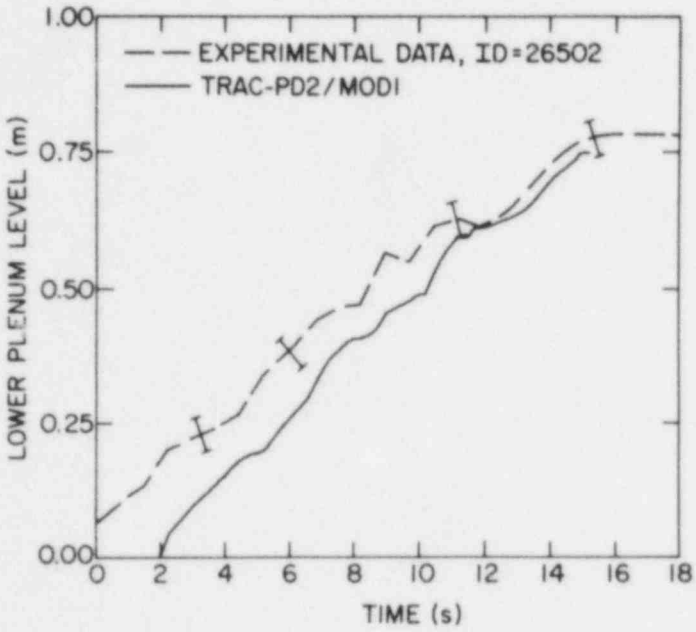

Figure 4.12 Comparison Between the TRAC-PD2/MOD1 Prediction and the Experimental Data for Lower Plenum Water Level for Test ID = 26502. (BNL Neg. No. 1-325-85)

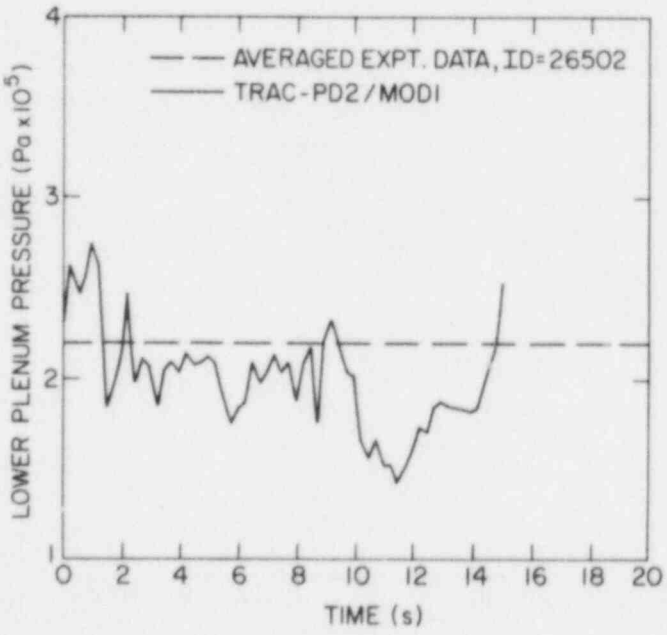

Figure 4.13 Comparison Between the TRAC-PD2/MOD1 Prediction and the Experimental Data for Lower Plenum Pressure for Test ID = 26502. (BNL Neg. No. 1-386-85)

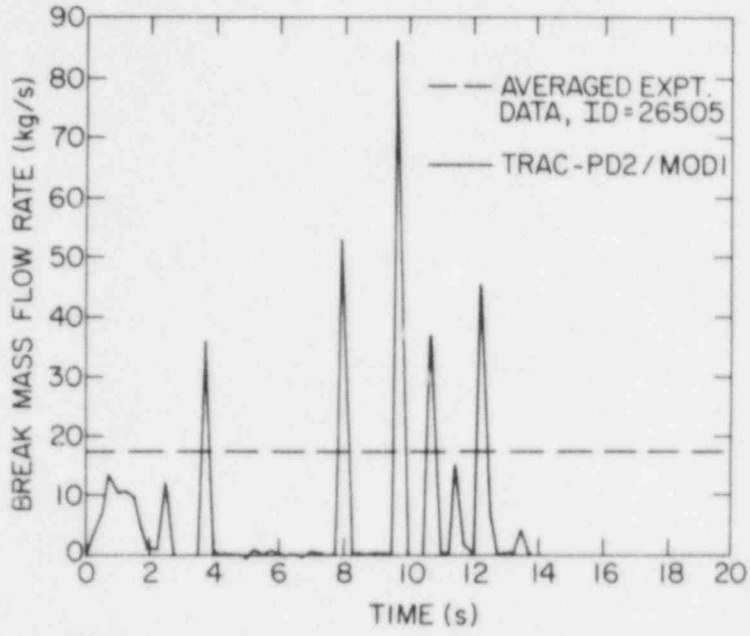

Figure 4.14 Comparison Between the TRAC-PD2/MOD1 Prediction and the Experimental Data for Break Mass Flow Rate for Test ID = 26505. (BNL Neg. No. 1-388-85)

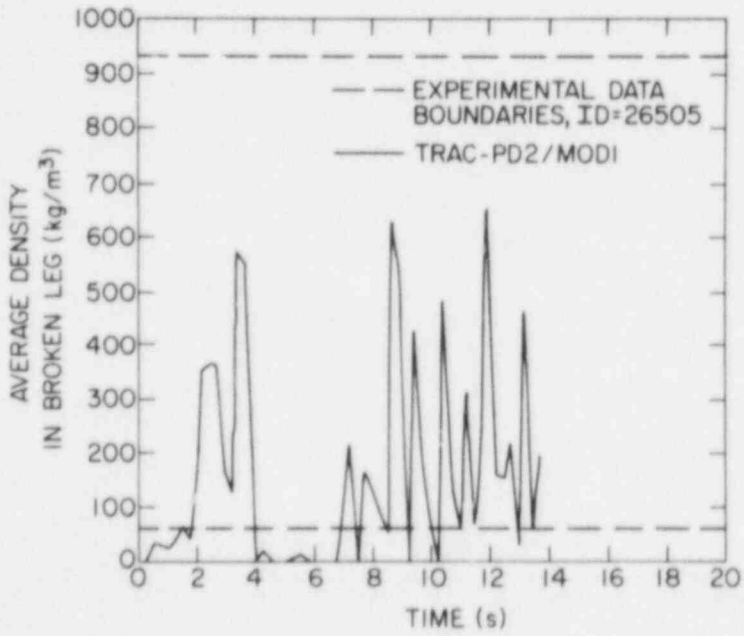

Figure 4.15 Comparison Between the TRAC-PD2/MOD1 Prediction and the Experimental Data for Average Fluid Density in Broken Leg for Test ID = 26505. (BNL Neg. No. 1-318-85)

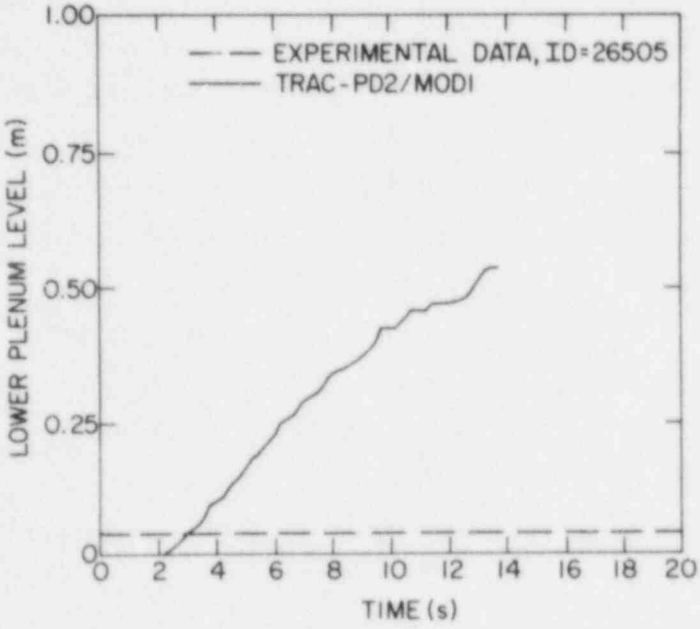

Figure 4.16 Comparison Between the TRAC-PD2/MOD1 Prediction and the Experimental Data for Lower Plenum Water Level for Test ID = 26505. (BNL Neg. No. 1-323-85)

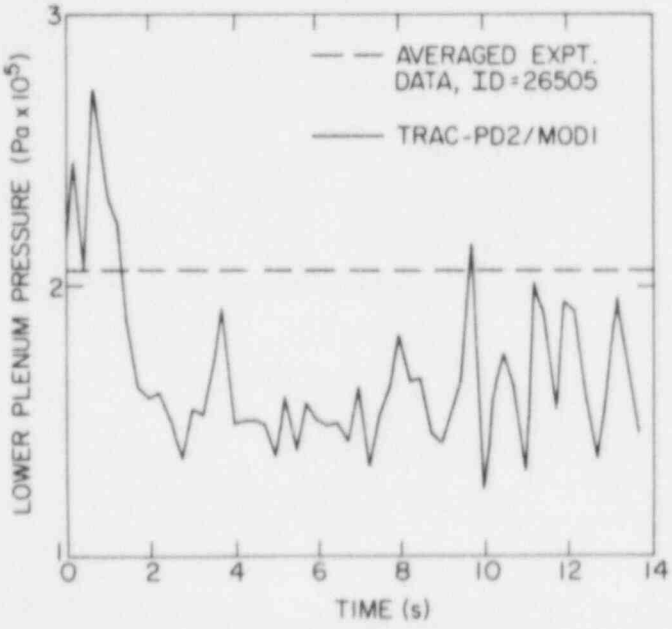

Figure 4.17 Comparison Between the TRAC-PD2/MOD1 Prediction and the Experimental Data for Lower Plenum Pressure for Test ID = 26505. (BNL Neg. No. 1-387-85)

A few more calculations were performed to study the code sensitivity to reverse core steam flow rate. Keeping everything the same as in the previous calculation for Test ID = 26505, the reverse core steam flow rate was increased in steps of 2% until the code predicted a complete bypass situation. With only a 4% increase in the steam flow rate, the code did predict a complete bypass condition. This demonstrates that for high ECC water subcooling (~95°C), TRAC-PD2/MOD1 may switch from an almost ECC-delivery to a complete ECC-bypass situation with just a slight increase in the reverse core steam flow. In other words, the code may predict an on-and-off-type ECC water delivery behavior for high ECC water subcooling typical during a large-break LOCA in PWRs. Finally, Figure 4.18 shows the comparison between the measured and predicted average water penetration rate for Test IDs = 26502 and 26505 including the sensitivity runs.

4.2 Transient Experiment

As mentioned earlier, the transient Test ID = 29302 with hot walls was also simulated with the TRAC-PD2/MOD1 (Version 27.0) code with BNL corrections. Also, three different modeling choices were made regarding the two hot leg plugs physically present in the downcomer annulus: (a) no hot leg plugs, (b) hot leg plugs inside cells, and (c) hot leg plugs on cell boundaries. A lumped-parameter heat slab model was used to simulate the vessel wall as this was the only option available in the TRAC-PD2/MOD1 (Version 27.0) code. The core steam flow rate and the containment pressure were specified as shown in Figure 2.2(a) and (b). ECC water injection at a rate of 22.52 kg/s began at 11.5s into the transient. Several key variables were monitored and they are compared with the experimental data in Figures 4.19 through 4.22.

Figure 4.19 shows the lower plenum water level as a function of time. Three TRAC predictions for water level (or plenum filling rate) were somewhat different from one another, but it is encouraging to see that all three calculations showed reasonable agreement with the data. The calculations did predict a delay in water penetration due to the hot wall effect, i.e., extra steam

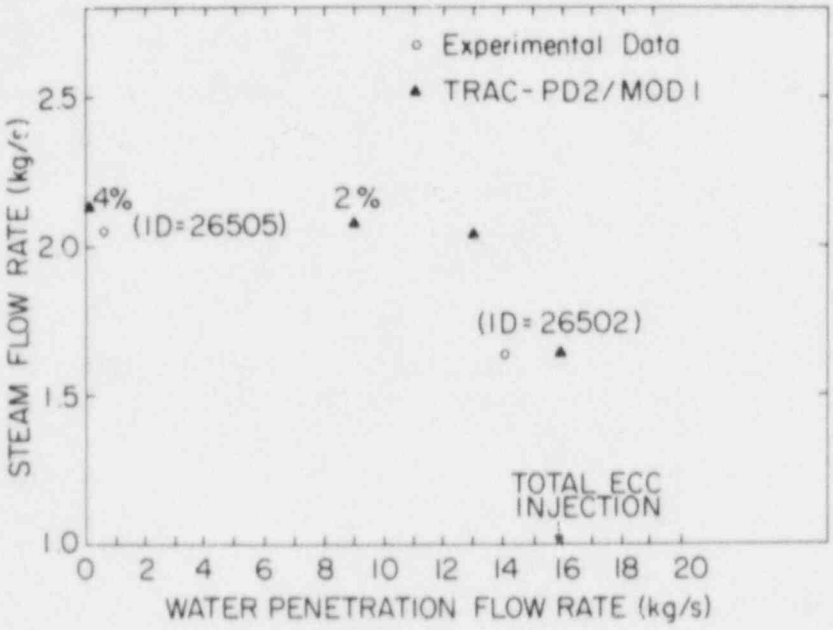

Figure 4.18 Comparison Between the TRAC-PD2/MOD1 Prediction (Including Sensitivity Calculations) and the Experimental Data for Average Water Penetration Rates for Test IDs = 26502 and 26505. (BNL Neg. No. 1-413-85)

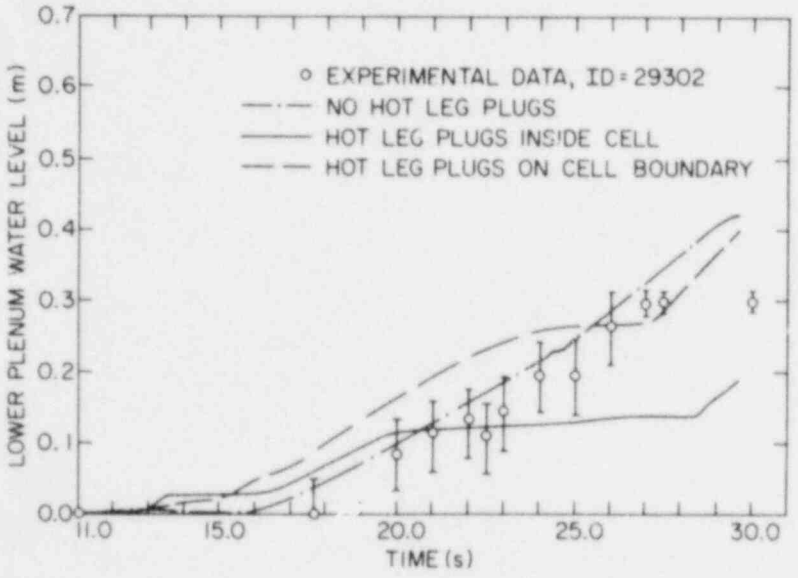

Figure 4.19 Comparison Between the TRAC-PD2/MOD1 Predictions and the Experimental Data for Lower Plenum Water Level for Test ID = 29302. (BNL Neg. No. 10-938-81)

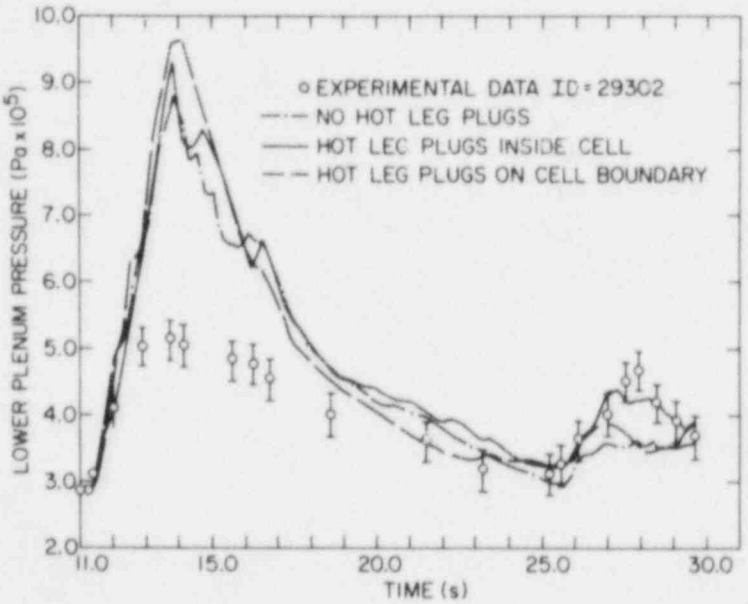

Figure 4.20 Comparison Between the TRAC-PD2/MOD1 Predictions and the Experimental Data for Lower Plenum Pressure for Test ID = 29302. (BNL Neg. No. 11-7-81)

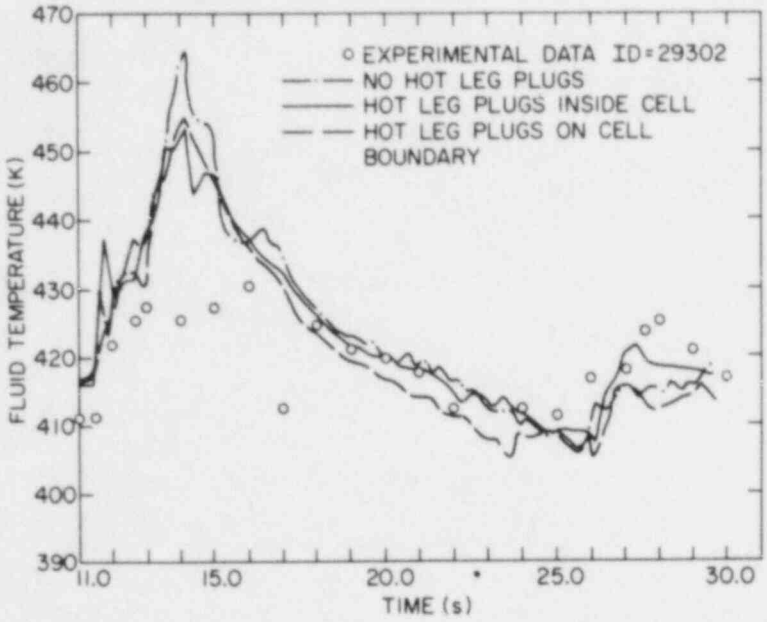

Figure 4.21 Comparison Between the TRAC-PD2/MOD1 Predictions and the Experimental Data for Downcomer Fluid Temperature for Test ID = 29302. (BNL Neg. No. 10-934-81)

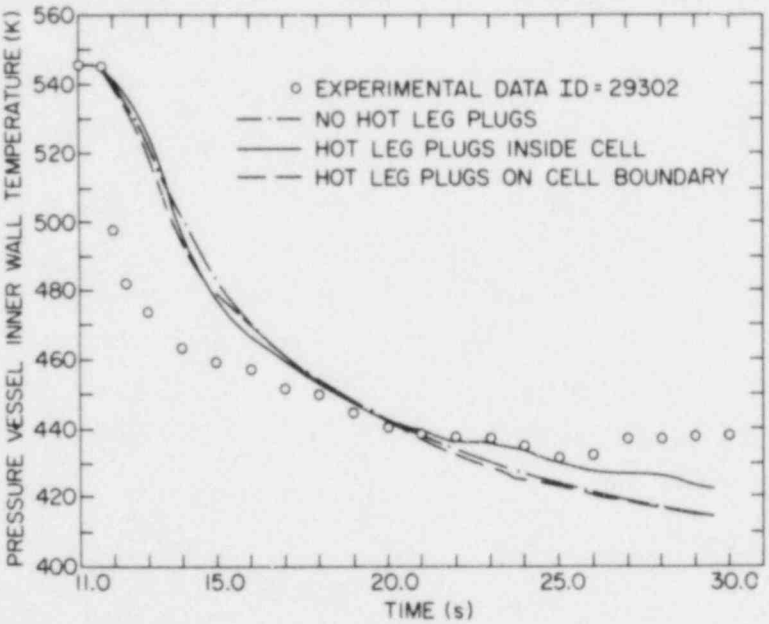

Figure 4.22 Comparison Between the TRAC-PD2/MOD1 Predictions and the Experimental Data for Vessel Inner Surface Temperature for Test ID = 29302. (BNL Neg. No. 10-937-81)

generation because of high initial wall temperature. The calculation with no hot leg plug shows an almost steady refill process, whereas the calculations with hot leg plugs (either inside the cells or on the cell boundaries) show variations in the filling rate with time. Furthermore, the calculation with the hot leg plugs on the cell boundaries yielded a larger refill rate than that with hot leg plugs inside the cells. This is to be expected, because in the former case, the hot leg plugs block the water flow in the azimuthal direction and help the water to flow downwards. This will be further discussed later in this section.

The predicted pressures in the lower plenum are compared to the measured values in Figure 4.20. The results of all three calculations were quite close to one another; however, all of them overpredicted the pressure during $12 < t < 20$s. The same trend can be seen in Figure 4.21 where the calculated volume-averaged fluid temperature in Cell 5 of Level 6 is compared to the experimental data. With some liquid in the cell, this temperature was only a few degrees above the saturation temperature corresponding to the pressure shown in Figure 4.20. Therefore, the calculations seem to be self-consistent, and the discrepancies are most probably due to the lumped conduction model for vessel heat slabs. Because of the lumped model, the heat transfer rate from the vessel wall was overpredicted which generated more steam and a higher pressure in the vessel. This notion is supported by Figure 4.22 where the predicted vessel surface temperature at axial Level 6, azimuthal Cell 5, is compared with the data. Because of the lumped treatment, the predicted surface temperature which is the same as the mean wall temperature remains higher than the data until $t > 20$s. Therefore, the driving potential for heat transfer, $T_{surface}-T_{fluid}$, is higher which results in the higher heat transfer rate and the higher pressure in the TRAC calculation.

As shown in Figure 4.19, the calculation with no hot leg plug indicates an almost steady filling rate, whereas the other two calculations show variations in the penetration rate. To improve our understanding of this behavior, the predicted liquid and steam flow directions in the downcomer annulus were mapped at various points in time.

Figures 4.23 and 4.24 show the predicted liquid and vapor flow directions and the void fraction distribution in the downcomer annulus (unwrapped) for no hot leg plugs at 18.4 and 22.4s, respectively. The water penetration rates were 9.8 and 11.9 kg/s, respectively. Both figures are quite similar regarding the flow directions and the void distribution. ECC water was predicted to be penetrated only through the azimuthal sector 5 which was diagonally opposite to the broken leg (located at azimuthal sector 7). Most of the water injected through the cold legs in azimuthal sectors 6 and 8 were predicted to flow in the azimuthal direction and out through the break because of steam updraft and proximity to the broken leg. The void fraction distribution also shows considerable water presence in the axial level 9 (although not completely filled with water) and in all levels in the azimuthal sector 5. Most of the other cells were almost completely filled with steam. It is interesting to note that steam was predicted to flow upwards in all azimuthal sectors except in the 5th sector where both co-current and countercurrent flow situations were predicted. In general, the predicted flow directions and void distributions look reasonable from a qualitative viewpoint, and the calculation demonstrated the multidimensional feature of the ECC-bypass phenomenon.

Figures 4.26 through 4.28 show similar maps for the TRAC calculation with the hot leg plugs inside the cells. It can be noted in Figure 4.19 that this calculation showed an extended period ($20 < t < 28.5$s) of little water penetration into the lower plenum. Before this period began, i.e., $t < 20$s, the flow behavior in the annulus was very similar to that without hot leg plugs. This can be seen by comparing Figure 4.25 where the results at t=18.32s are shown, with Figures 4.23 and 4.24. However, at $t > 20$s, the water bypass rate increased and the flow behavior in the annulus changed significantly. This is shown in Figures 4.26 and 4.27 where the flow directions and void fractions are mapped for $t = 22.29$ and $t = 26.42$s, respectively. Notice that there was

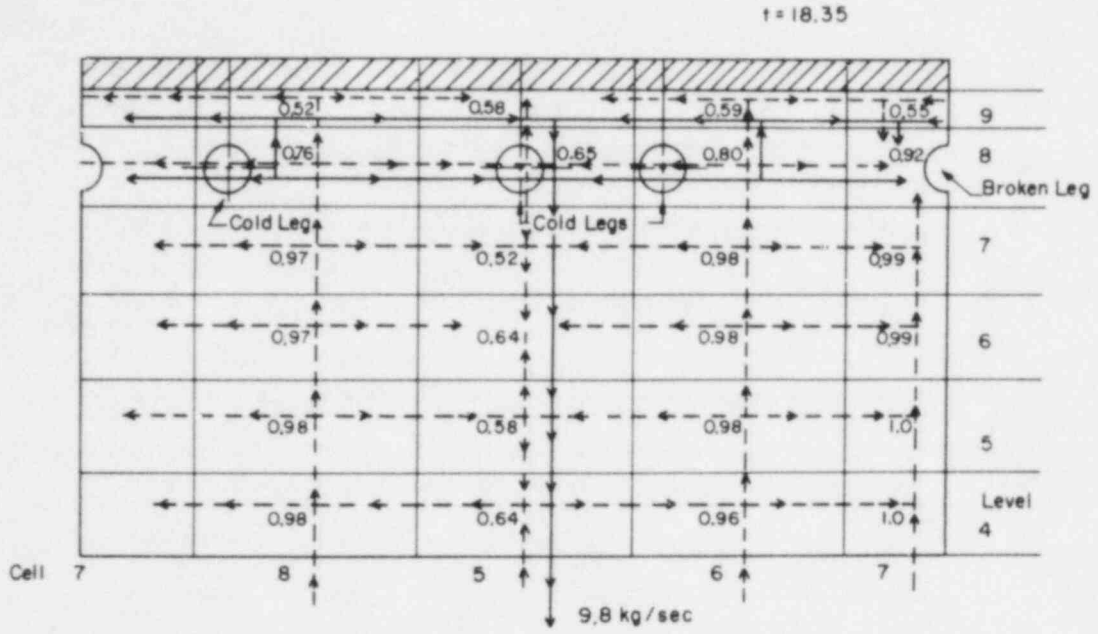

Figure 4.23 TRAC-PD2/MOD1 Liquid (——) and Vapor (---) Flow Directions and Void Fractions in Downcomer at 18.35 Second for Test ID = 29302. (BNL Neg. No. 12-309-81)

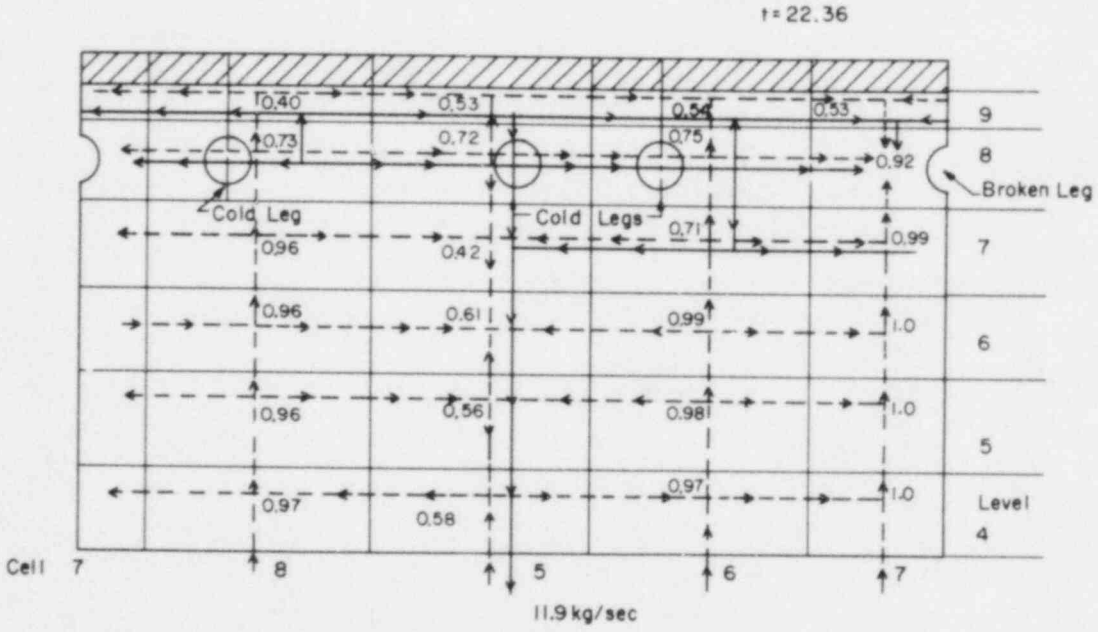

Figure 4.24 TRAC-PD2/MOD1 Liquid (——) and Vapor (---) Flow Directions and Void Fractions in Downcomer at 22.36 Second for Test ID = 29302. (BNL Neg. No. 12-307-81)

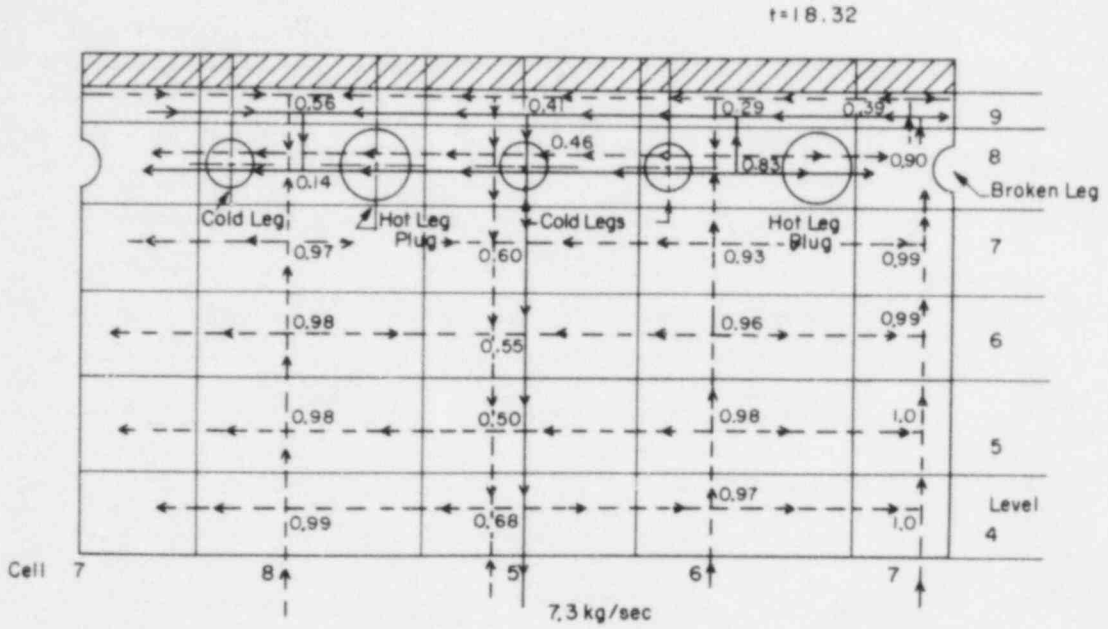

Figure 4.25 TRAC-PD2/MOD1 Liquid (——) and Vapor (---) Flow Directions and Void Fractions in Downcomer at 18.32 Second for Test ID = 29302. (BNL Neg. No. 12-305-81)

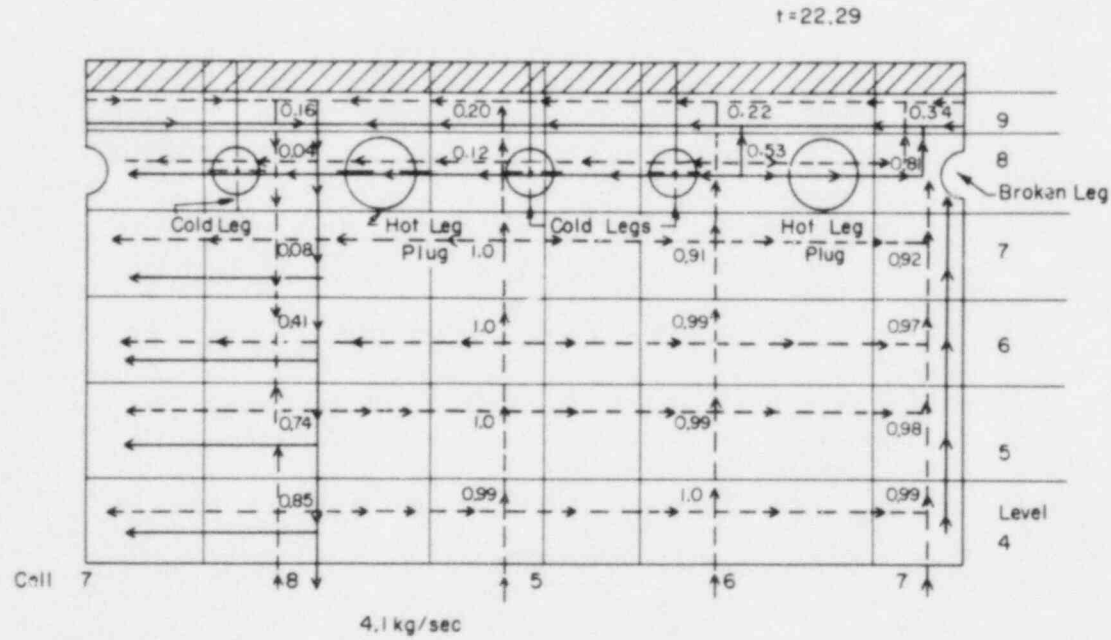

Figure 4.26 TRAC-PD2/MOD1 Liquid (——) and Void (---) Flow Directions and Void Fractions in Downcomer at 22.29 Second for Test ID = 29302. (BNL Neg. No. 12-306-81)

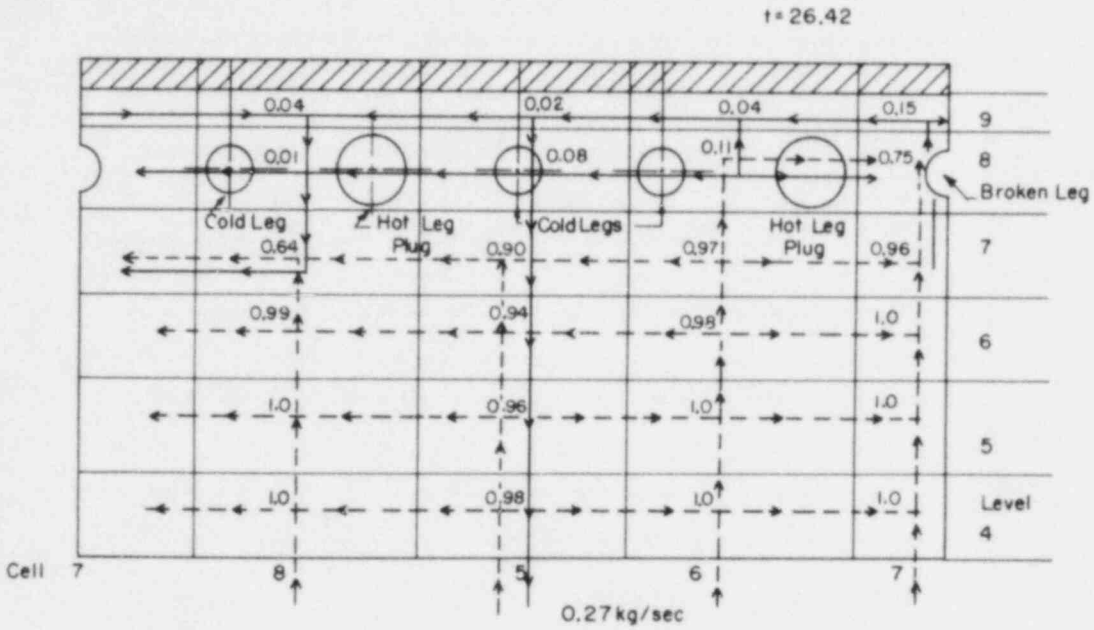

Figure 4.27 TRAC-PD2/MOD1 Liquid (——) and Vapor (---) Flow Directions and Void Fractions in Downcomer at 26.42 Second for Test ID = 29302. (BNL Neg. No. 12-313-81)

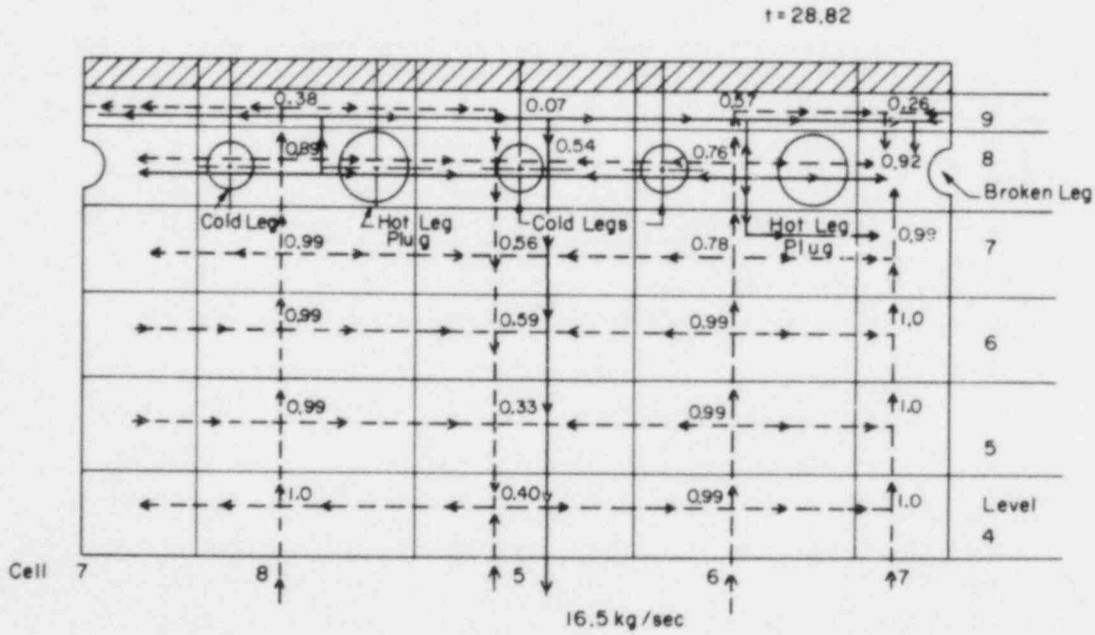

Figure 4.28 TRAC-PD2/MOD1 Liquid (——) and Vapor (---) Flow Directions and Void Fractions in Downcomer at 28.82 Second for Test ID = 29302. (BNL Neg. No. 12-311-81)

significant storage of water in the upper levels of the downcomer. The small amount of water that was able to penetrate was either through the 8th or 5th azimuthal sector. At t = 28.5s, the ECC water began to penetrate again and the flow behavior became similar to that at t < 20s. This can be seen by comparing Figures 4.25 and 4.28. It should be noticed that during significant water penetration (Figures 4.25 and 4.28), the flow is mostly co-current downwards in the 5th azimuthal sector, whereas it is mostly countercurrent in the same sector during ECC bypass (Figure 4.27).

Finally, the flow directions and the void fraction distribution for the calculation with hot leg plugs on the cell boundaries are shown in Figures 4.29 through 4.32 for t = 18.31, 22.29, 26.51, and 27.71s, respectively. Since the plugs were blocking 98% of the flow area in the azimuthal direction (at axial Level 8) between Cells 8 and 5, and Cells 6 and 7, very little water or steam could flow across these boundaries. This created an adverse condition for the ECC water bypass, and thus a favorable situation for water penetration into the lower plenum. This explains why the lower plenum filling rate for this calculation is larger than that for the hot leg plugs inside cells (see Figure 4.19). As before, the flow directions and void fraction distribution look reasonable qualitatively, and the calculation shows the multidimensional feature of the ECC-bypass phenomenon.

In spite of TRAC's success in predicting a reasonable plenum filling rate for Test ID = 29302, a number of unresolved issues remain. For example, which of the three choices for modeling the physically present hot leg plugs or penetrations should be recommended? Why did the TRAC prediction for lower plenum water level keep rising even though the steam flow rate was raised at t = 26s and the data showed a constant level beyond 27s (see Figure 4.19)? Why did TRAC predict a reasonable penetration rate even though the wall-to-fluid heat transfer rate and the extra steam generation rate were probably higher than that in the test?

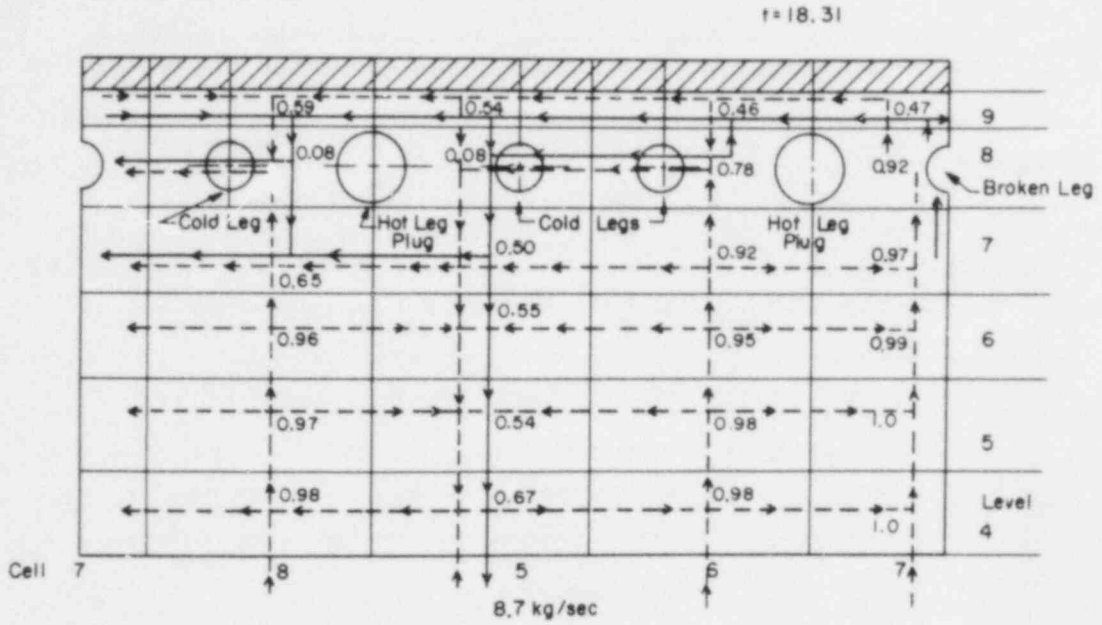

Figure 4.29 TRAC-PD2/MOD1 Liquid (——) and Vapor (---) Flow Directions and Void Fractions in Downcomer at 18.31 Second for Test ID = 29302. (BNL Neg. No. 12-310-81)

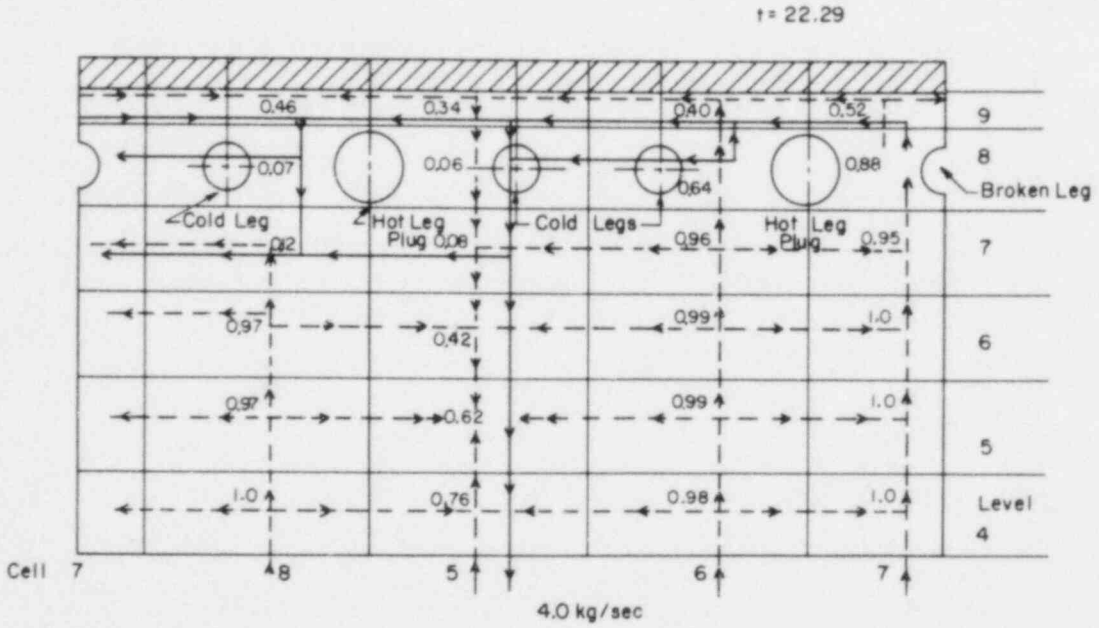

Figure 4.30 TRAC-PD2/MOD1 Liquid (——) and Vapor (---) Flow Directions and Void Fractions in Downcomer at 22.29 Second for Test ID = 29302. (BNL Neg. No. 12-308-81)

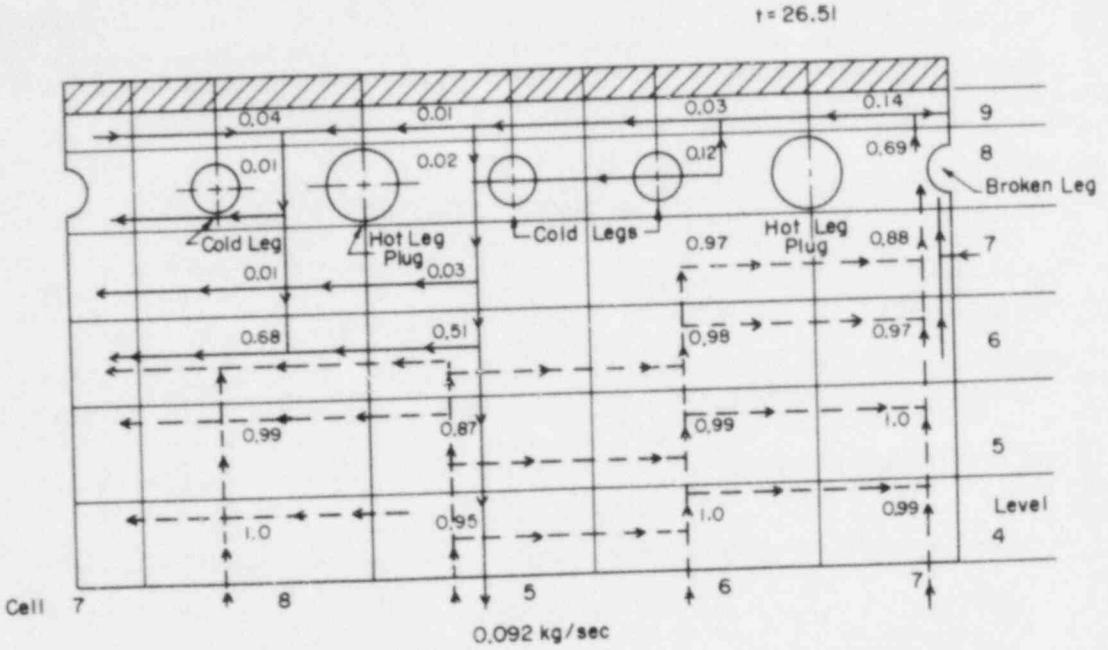

Figure 4.31 TRAC-PD2/MOD1 Liquid (——) and Vapor (---) Flow Directions and Void Fractions in Downcomer at 26.51 Second for Test ID = 29302. (BNL Neg. No. 12-304-81)

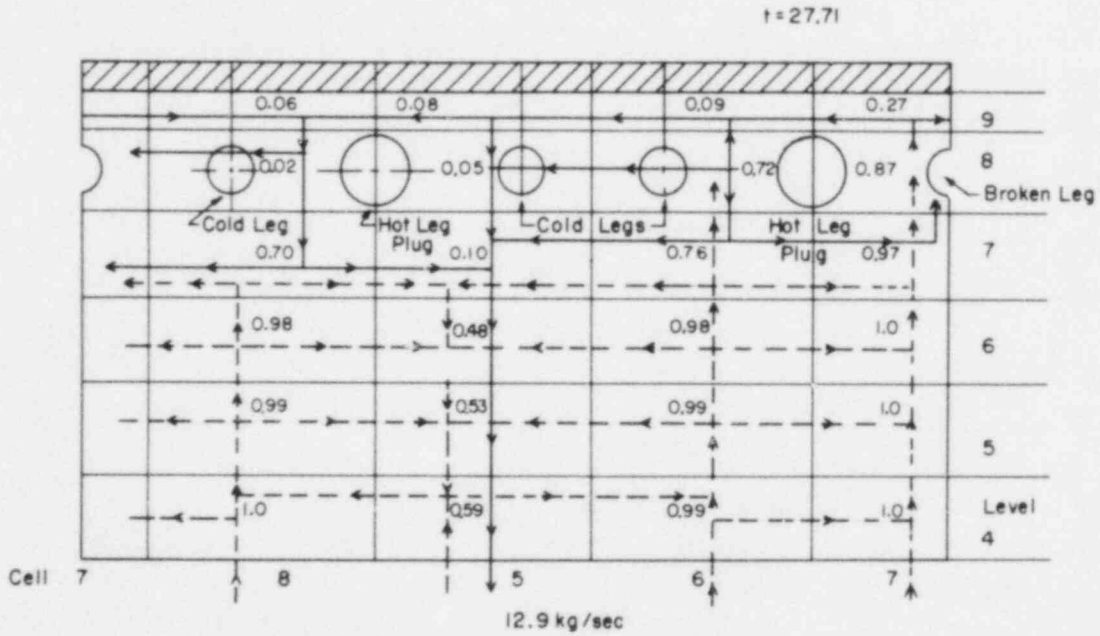

Figure 4.32 TRAC-PD2/MOD1 Liquid (——) and Vapor (---) Flow Directions and Void Fractions in Downcomer at 27.71 Second for Test ID = 29302. (BNL Neg. No. 12-306-81)

Some of these issues were further investigated by using a one-dimensional (radial) heat conduction model for the vessel wall instead of the lumped model. This was achieved by incorporating the appropriate UPDATEs received from LANL. The transient test (ID=29302) was rerun with five radial nodes in the vessel wall. Also, the nodalization used for the steady-state experiments, i.e., the hot leg plugs blocking 50% of the azimuthal flow area in Level 8, was added. Thus four different hot leg plug positions were considered: (a) no hot leg plugs, (b) hot leg plugs inside cells, (c) hot leg plugs on cell boundaries, and (d) hot leg plugs blocking 50% of the azimuthal flow area. The results of these calculations are shown in Figures 4.33 and 4.34.

Since the one-dimensional model gives a much better representation of the heat transfer from vessel wall to the downcomer fluid, good agreement between the code calculations and the data for lower plenum pressure was achieved as shown in Figure 4.33. However, the lower plenum filling rate was significantly overpredicted as shown in Figure 4.34. Furthermore, there were large differences in the calculated filling rates depending on the location of the hot leg plugs relative to the azimuthal cell boundaries. These results raised more concern on how to model the hot leg plugs in the TRAC framework. Therefore, further investigations were carried out at BNL, and these will be discussed in Chapter 5.

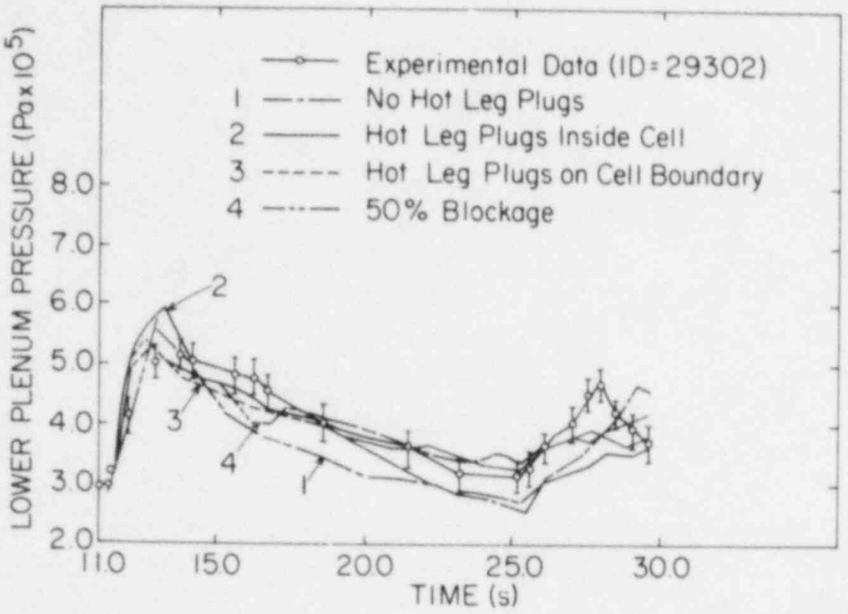

Figure 4.33 Comparison Between the TRAC-PD2/MOD1 Predictions with 1-D Vessel Wall Conduction and the Experimental Data for Lower Plenum Pressure for Test ID = 29302. (BNL Neg. No. 1-411-85)

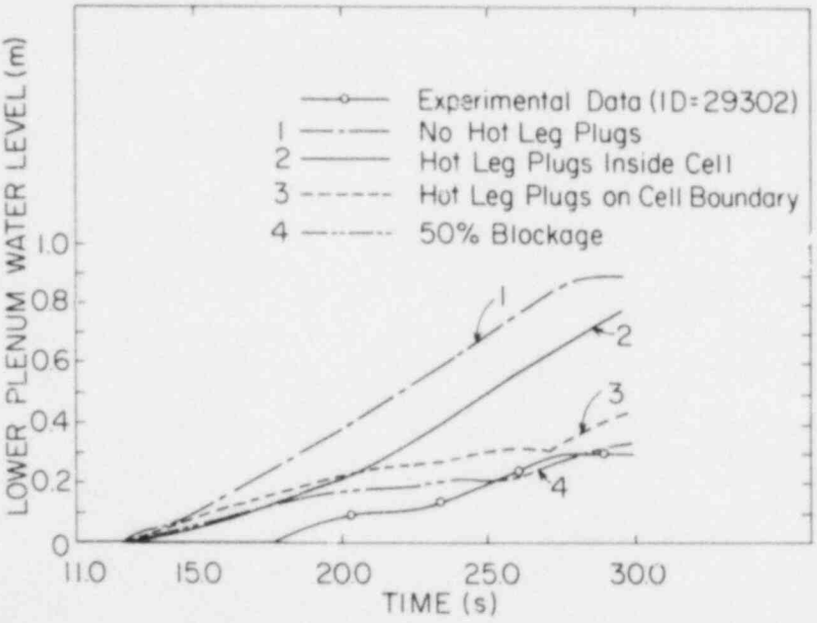

Figure 4.34 Comparison Between the TRAC-PD2/MOD1 Predictions with 1-D Vessel Wall Conduction and the Experimental Data for Lower Plenum Water Level for Test ID = 29302. (BNL Neg. No. 1-422-85)

5. FURTHER ANALYSIS AND DISCUSSION

The base calculations presented in Chapter 4 show reasonable agreement between the TRAC-PD2/MOD1 predictions and the test data. However, the code results are very sensitive to the location of the hot leg plugs relative to the azimuthal cell boundaries. Even conflicting results have been obtained for the same nodalization, as shown in Figures 4.19 and 4.34. Thus, it was imperative to further investigate the effect of nodalization. [It should be noted that the LANL staff usually neglects the presence of hot leg plugs or the hot leg penetrations in their downcomer models when studying the ECC-bypass phenomenon. However, hot leg pipes do penetrate through the downcomer annulus in full-scale reactors, and thus the BCL 2/15-scale vessel provides a better representation of the real situation than the Creare vessels (Crowley, 1977) without the hot leg plugs. It is also felt that a best-estimate code such as TRAC ought to be able to take into account the presence of hot leg plugs or penetrations. Moreover, a complete analysis including the hot leg penetrations is required to arrive at an effective set of user guidelines for full-scale reactor applications.]

Two sensitivity studies were performed. First, the steady-state experiments (Test IDs = 26716, 26719, 26502, and 26505) were rerun with the following four possible hot leg plug locations relative to the azimuthal cell boundaries: (a) no hot leg plugs, (b) hot leg plugs inside cells, (c) hot leg plugs on cell boundaries, and (d) hot leg plugs blocking 50% of azimuthal flow area. The base case calculations performed using this last nodalization, i.e., Case (d), were presented in Section 4.1. The second sensitivity study was performed by renodalizing the upper part of the downcomer. In this new nodalization, the axial Levels 9, 8 and part of Level 7 of the base nodalization, as shown in Figure 3.1, were lumped together to form one axial level. Thus, the new nodalization had eight axial levels. The results of these two studies will now be discussed separately.

Figure 5.1 shows the various locations of the hot leg plugs relative to the azimuthal cell boundaries. Nine axial levels, as shown in Figure 3.1, were

1) No plugs

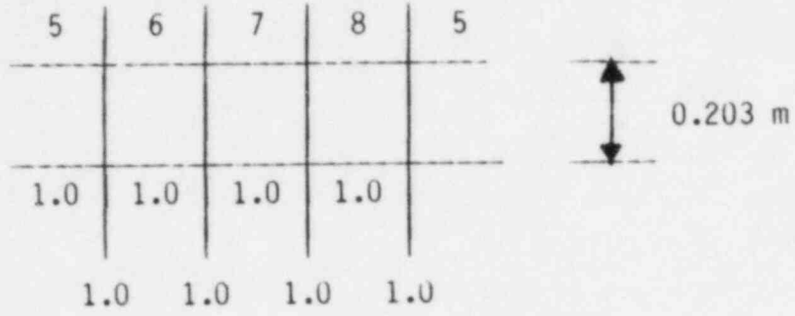

2) Plugs inside a volume

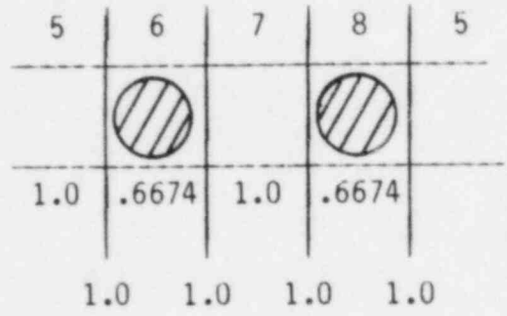

3) Hot leg plugs on boundary

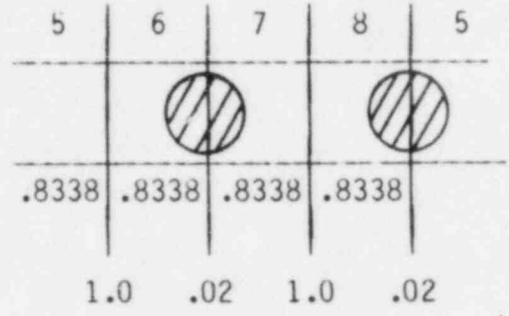

4) 50% blockage on boundary

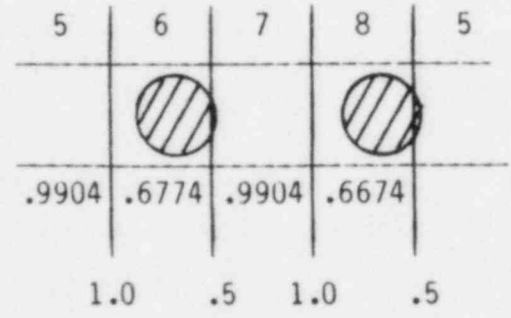

Figure 5.1 Hot Leg Plug Representations (9 Level Vessel)

used. The cell fluid volume fractions (Vol. FRAC) and the flow areas in the azimuthal direction (FA-T) for axial Level 8 (where the hot leg plugs were physically located) are also shown in Figure 5.1. Figures 5.2 through 5.5 show the comparisons between the predicted and measured lower plenum water levels for the steady-state experiments mentioned earlier. The TRAC results are indeed very sensitive to the presence of hot leg plugs and their locations relative to the cell boundaries. Besides, no clear trend emerged; thus it is difficult to provide user guidelines as to the relative location of hot leg penetrations for analysis of full-scale PWRs.

For the second sensitivity study, eight axial levels were used. The eighth level was comprised of the ninth, eighth and part of the seventh level of the base nodalization. The height of this level was 0.402 m, approximately twice the diameter of the hot leg plugs. Three different relative locations of the plugs were studied: (a) no hot leg plugs, (b) plugs inside cells, (c) plugs on the azimuthal cell boundaries. Figure 5.6 shows the fluid volume fractions (Vol. FRAC) and the azimuthal flow areas (FA-T) associated with this new nodalization.

Figures 5.7 and 5.8 show the comparison between the predicted and measured data for lower plenum water levels for Test IDs = 26716 and 26719, respectively. For these tests, the code results for all three different hot leg plug representations were close to each other. However, they all significantly overpredicted the test data and showed different trends when compared to the 9-level results shown in Figures 5.2 and 5.3. For experiments with high ECC water subcooling, i.e., Test ID = 26502, the code underpredicted the water filling rate (see Figure 5.9). For Test ID = 26505, however, the code did predict a complete bypass, i.e., no water filling, in agreement with the test.

The transient test (ID = 29302) was also rerun with the 8-level vessel model and one-dimensional heat conduction in the vessel wall. The predicted lower plenum water levels for various hot leg plug representations are shown in Figure 5.10 along with the data. Reasonable agreement with the data has been

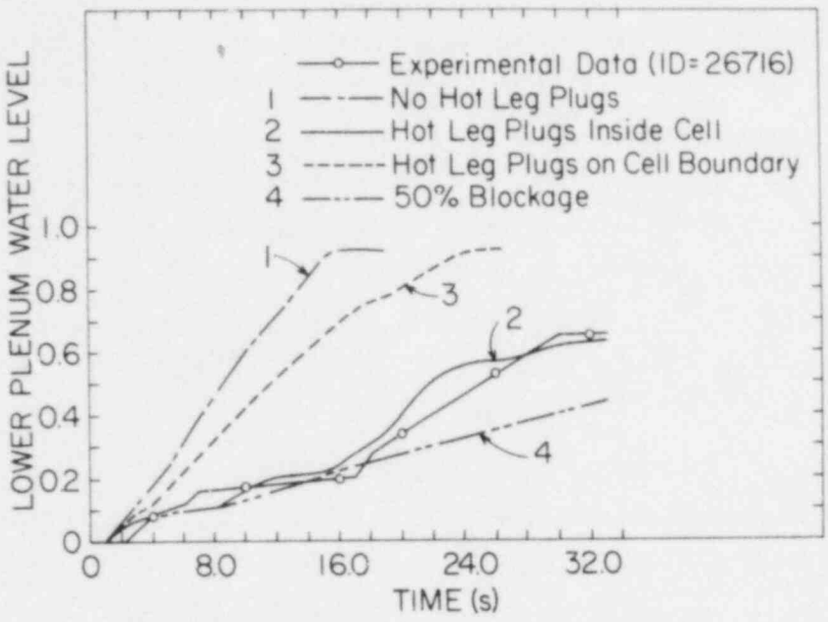

Figure 5.2 Comparison Between the TRAC-PD2/MOD1 Predictions and the Experimental Data for Lower Plenum Water Level for Test ID = 26716. (BNL Neg. No. 1-418-85)

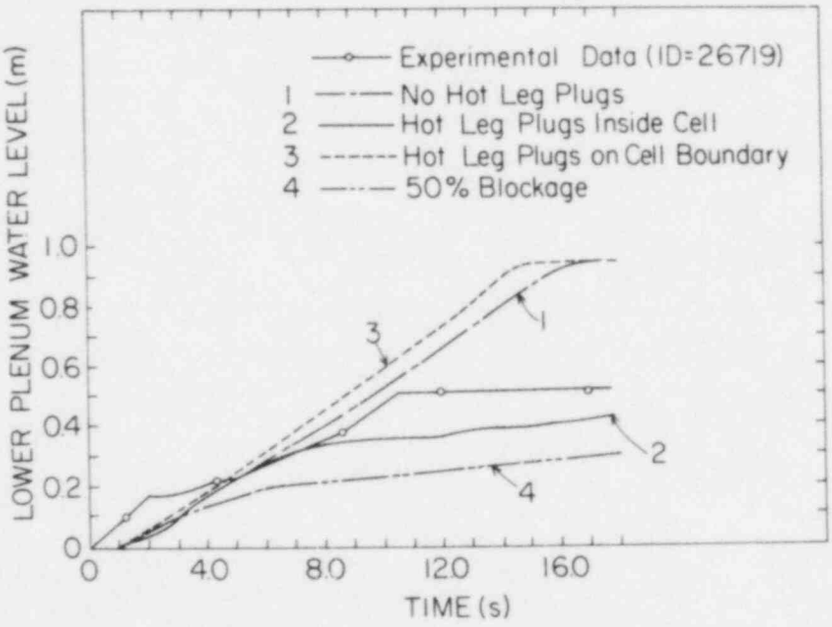

Figure 5.3 Comparison Between the TRAC-PD2/MOD1 Predictions and the Experimental Data for Lower Plenum Water Level for Test ID = 26719. (BNL Neg. No. 1-417-85)

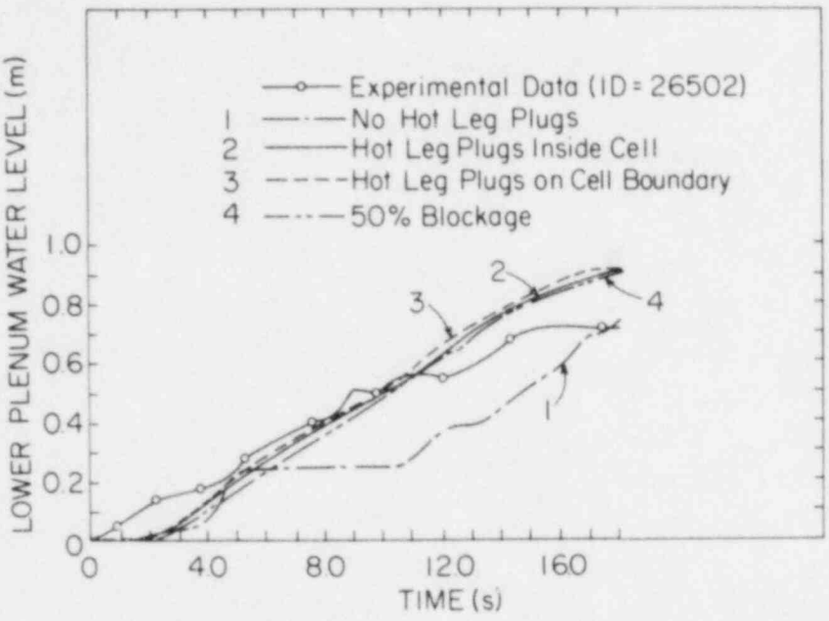

Figure 5.4 Comparison Between the TRAC-PD2/MOD1 Predictions and the Experimental Data for Lower Plenum Water Level for Test ID = 26502. (BNL Neg. No. 1-419-85)

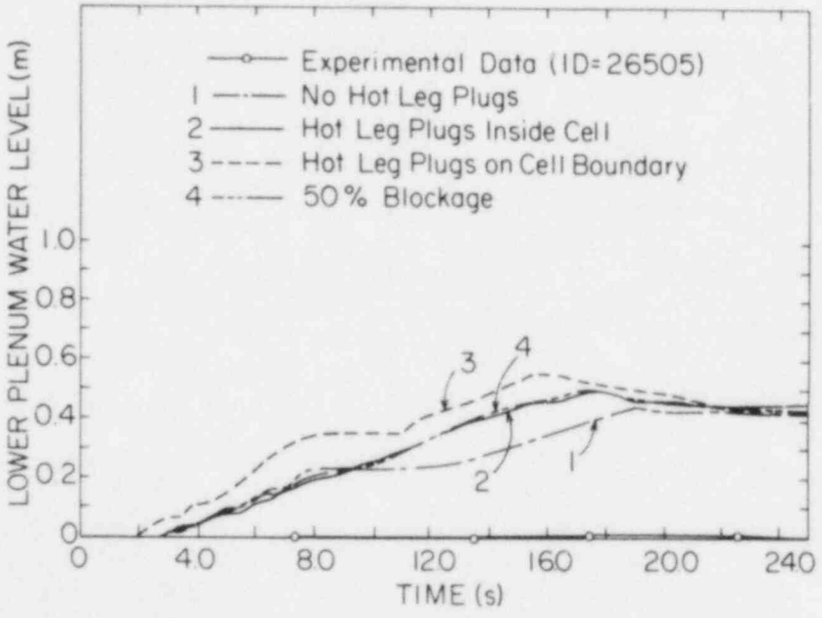

Figure 5.5 Comparison Between the TRAC-PD2/MOD1 Predictions and the Experimental Data for Lower Plenum Water Level for Test ID = 26505. (BNL Neg. No. 1-421-85)

1) No plugs

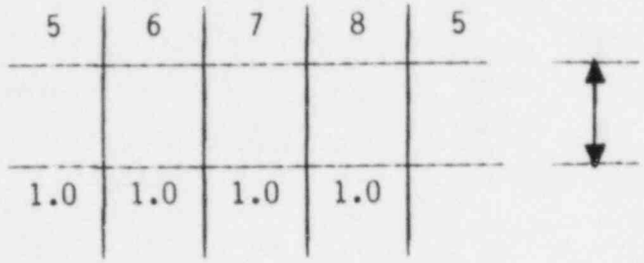

2) Plugs inside volumes

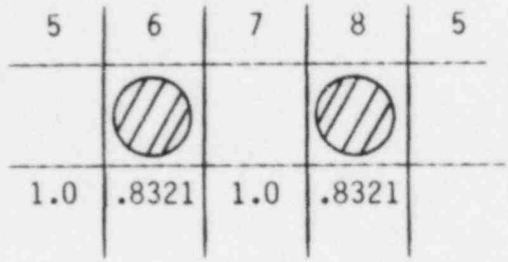

3) Plugs in cell boundary

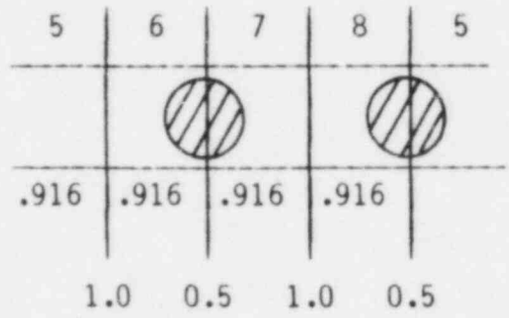

(Numbers are selected to reference the "similar" 9 level vessel)

Figure 5.6 Hot Leg Plug Representations (8 Level Vessel)

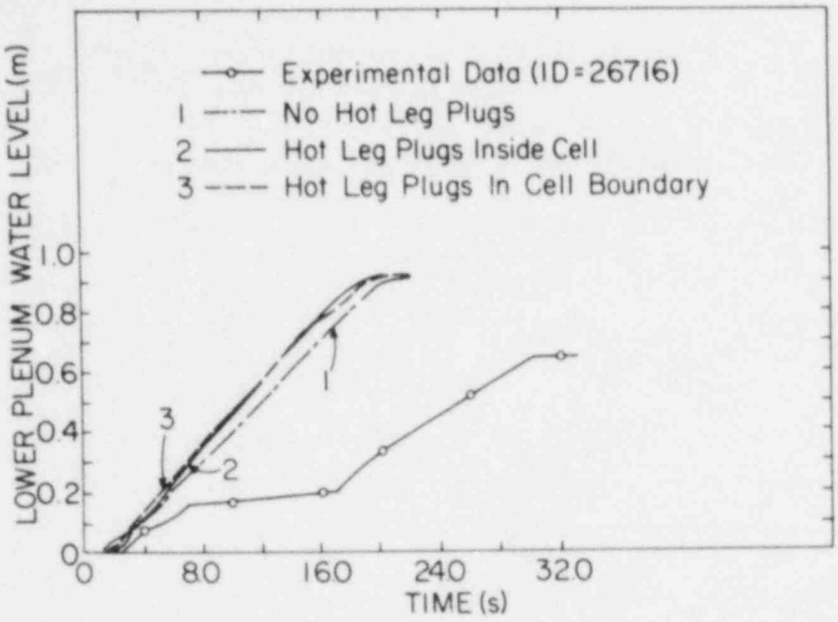

Figure 5.7 Comparison Between the TRAC-PD2/MOD1 Predictions (with 8-Level Vessel) and the Experimental Data for Lower Plenum Water Level for Test ID = 26716. (BNL Neg. No. 1-655-85)

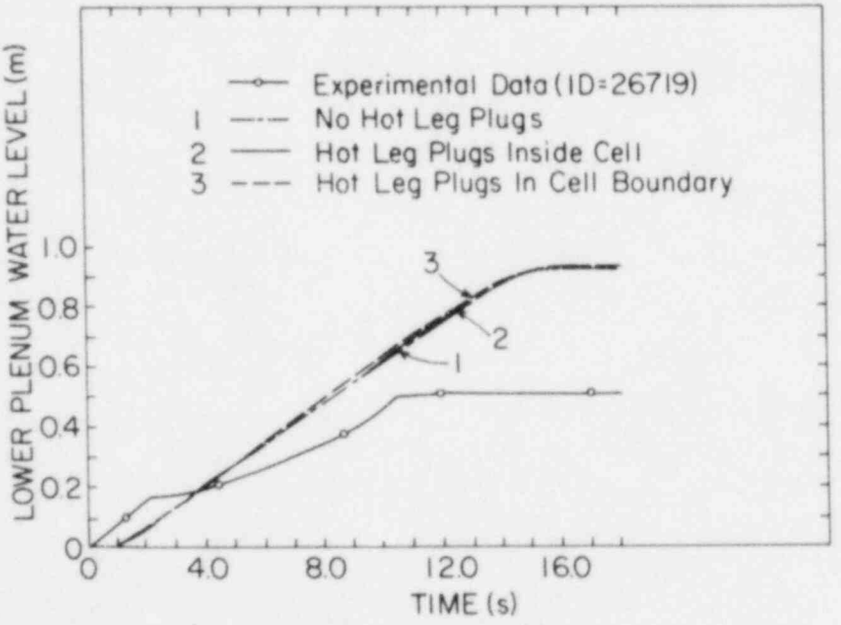

Figure 5.8 Comparison Between the TRAC-PD2/MOD1 Predictions (with 8-Level Vessel) and the Experimental Data for Lower Plenum Water Level for Test ID = 26719. (BNL Neg. No. 1-657-85)

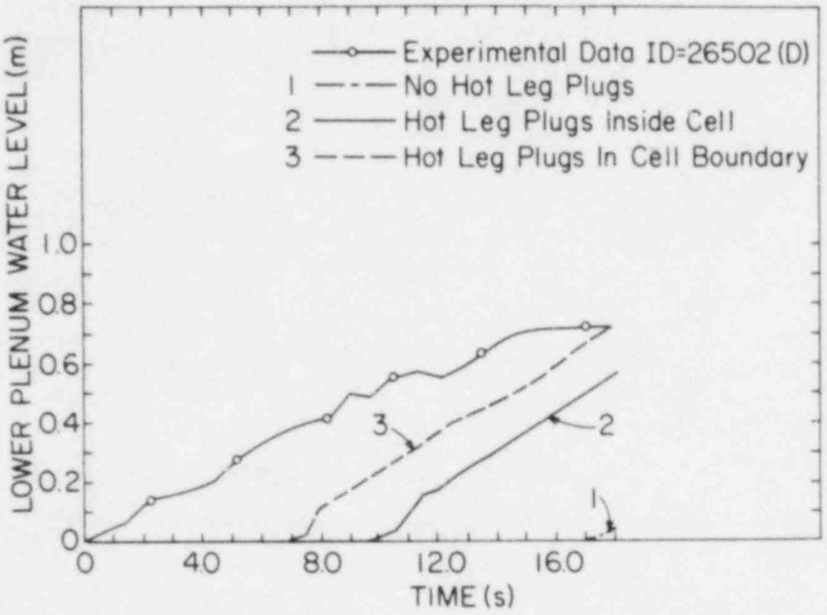

Figure 5.9 Comparison Between the TRAC-PD2/MOD1 Predictions (with 8-Level Vessel) and the Experimental Data for Lower Plenum Water Level for Test ID=26502. (BNL Neg. No. 1-658-85)

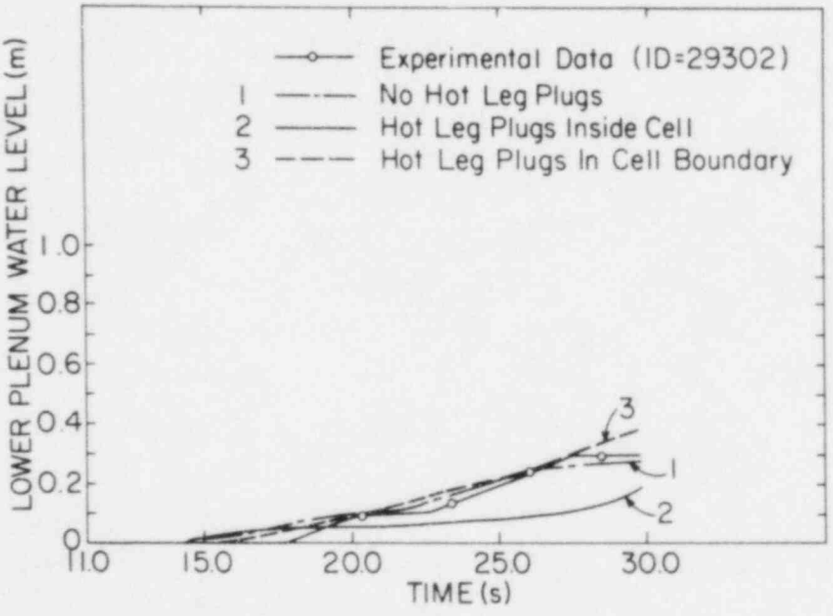

Figure 5.10 Comparison Between the TRAC-PD2/MOD1 Predictions (with 8-Level Vessel and 1-D Vessel Wall Conduction) and the Experimental Data for Lower Plenum Water Level for Test ID = 29302. (BNL Neg. No. 1-656-85)

found for two hot leg plug representations. However, the results are quite different from that obtained using the 9-level base nodalization (see Figure 4.34 for comparison).

Results of the above two sensitivity studies were so confusing, and sometimes contradictory, that no effective user guidelines could be developed without further work for a full-scale PWR LOCA analysis. The code developers at LANL were informed of these results (Saha, 1982b), and independent parallel efforts were continued at BNL to uncover any hidden mistakes either in the code or in the input model.

During the check-out process at BNL, a steady-state TRAC-PD2/MOD1 calculation for a simple annulus test section with only one axial level was carried out. The input deck was essentially that of the eighth level of the base input deck with no flow in the axial direction. There were four azimuthal sectors, and no hot leg plugs in the model. In each sector, a PIPE component was attached; three were for water injection while the fourth was the broken leg. The water injection rates and exit (broken leg) pressure were taken from the BCL test ID = 26716, but the water temperature was reduced so that a single-phase water condition existed throughout the test section.

The results of this simple test were rather disturbing. The TRAC-PD2/MOD1 code, with or without the UPDATE for a momentum term ($V_z \partial V_\theta / \partial z$) correction, predicted an asymmetric flow distribution around the annulus in spite of the symmetric boundary condition. For the particular test run, the cell opposite to the broken leg divided its flow into 1.7 kg/s in one direction and 6.0 kg/s in the other. This input deck and the results were also sent to the code developers at LANL for examination. A code error in wall friction in the azimuthal direction was found by the LANL staff and the appropriate UPDATE was sent to BNL to correct the asymmetric flow split problem.

The BCL Test ID = 26716 was rerun with all the corrections received from LANL. The base case nodalization with four different hot leg plug representations as shown in Figure 5.1 were used. The new predictions (designated by N) along with the old predictions (i.e., before the latest UPDATE set) and

the test data are shown in Figure 5.11. It can be seen that the code predictions for the refill rate have changed for all four cases. However, the proper order, at least from an intuitive viewpoint, has not been achieved. For example, the calculation with the hot leg plugs on the boundary (i.e., Curve 3 in Figure 5.11) has changed from an almost complete delivery case to an almost complete bypass event (i.e., curve 3N in Figure 5.11). Intuitively, both curves should have predicted the highest refilling rate, since this nodalization represents the maximum amount of blockage in the azimuthal direction. Also, the new predictions showed a trend of decreasing the refill rate except for the case with the hot leg plugs inside the cell (i.e., Curve 2N in Figure 5.11). This does not seem to be correct from an intuitive viewpoint either.

To continue the analysis, more calculations were performed by taking into account the form losses produced by the hot leg plugs. The drag coefficient for flow around a circular cylinder was used for this purpose. For Reynolds number in the 100 to 200,000 range, a value of 1.2 may be taken as the drag coefficient (Schlichting, 1968). The additive loss coefficient for each plug, as required by TRAC, was computed as

$$FRIC = \frac{C_D A_p}{2(Vol)} = 1.275 m^{-1}$$

where A_p is the projected area of a plug in the flow direction and Vol is the volume of the cell. Since the liquid inertia ($\rho_\ell v^2_\ell$) is much larger than that of the vapor ($\rho_v v^2_v$), the additive loss coefficient was added only to the liquid phase. For the cases where a plug occupied space in two adjacent cells, the additive loss coefficient was split according to the volume fraction occupied by the plug in these cells. The results of the prediction can be found in Figure 5.12 with the letter K designating the calculations with the additive loss coefficients and the code corrections. (The curves with the letter N were obtained by the corrected code, but without the additive loss coefficients, and are the same as shown in Figure 5.11.)

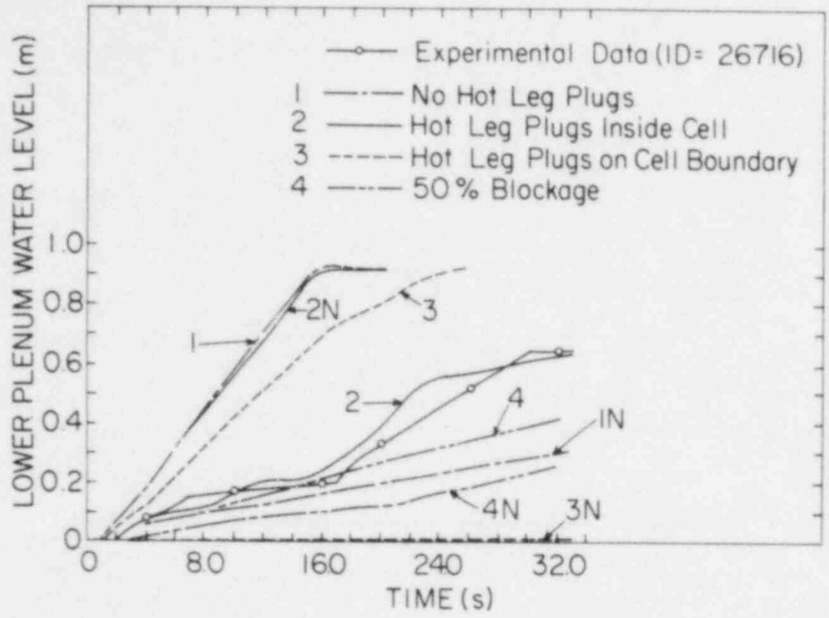

Figure 5.11 Comparison of the TRAC-PD2/MOD1 Predictions (Original and Updated) with the Experimental Data for Lower Plenum Water Level for Test ID = 26716. (BNL Neg. No. 1-422-85)

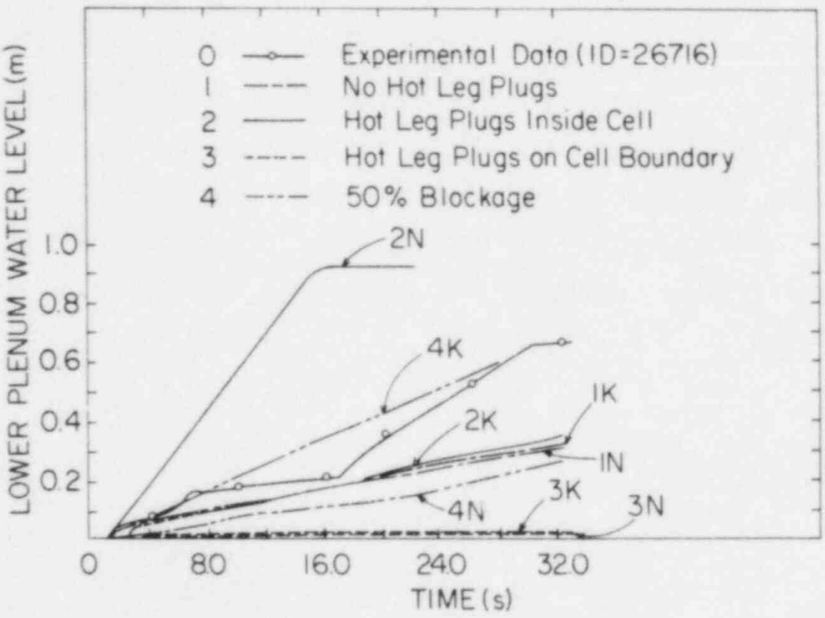

Figure 5.12 Comparison of Updated TRAC-PD2/MOD1 Predictions (With and Without Form Losses) With the Experimental Data for Lower Plenum Water Level for Test ID = 26716. (BNL Neg. No. 1-414-85)

It can be seen that even these new calculations with the additive loss coefficients are not consistent with each other. For hot leg plugs on the boundary (Case 3) and no hot leg plugs (Case 1), the results with the additive frictional losses changed very little from the calculations without the additive friction. For Cases 2 and 4, changes were significant although they were in opposite directions. For example, the liquid filling rate decreased for the case of plug inside the volume (Case 3), whereas the liquid filling rate increased for Case 4 which assumes 50% blockage on the azimuthal cell boundary. These results seem to have no physical basis and follow no recognizable trend which could be used in formulating user guidelines.

In summary, the TRAC-PD2/MOD1 code (Version 27.0) with BNL corrections may provide reasonable agreement with the ECC-bypass data as shown in Chapter 4. However, good agreement could be fortuitous since the TRAC results are so sensitive to nodalization at the upper downcomer region and the relative location of the hot leg penetrations. Even with the corrections for wall friction in the azimuthal direction and momentum term $V_z \partial V_\theta / \partial z$, and additive loss coefficients for hot leg plugs, the code results were not consistent as shown in Figures 5.11 and 5.12. Also, small variation in input numbers produced a large change in the code output. The code developers at LANL also experienced such sensitivity (Liles, 1983). As a result, no accuracy statement or user guidelines can be provided on the basis of the present work. It is suggested that the code developers at LANL reexamine the code, including its constitutive package, and improve the consistency of code prediction for the analysis of ECC-bypass phenomenon.

6. CONCLUSIONS AND RECOMMENDATIONS

From the results reported in Chapters 4 and 5, we draw the following major conclusions:

1. The TRAC-PD2/MOD1 code may predict the ECC bypass (or ECC delivery into the lower plenum) during a PWR large-break LOCA with reasonable success. However, the code results are highly sensitive to nodalization and the relative locations of the hot leg penetrations in the downcomer annulus. This precludes making any firm statement about the code accuracy and providing user guidelines for PWR LOCA studies.

2. The code does calculate a strong multidimensional thermal-hydraulic behavior expected in a PWR downcomer during the refill stage of a large break LOCA. Thus, the code has the potential to be a very useful tool for best-estimate or realistic analysis of PWR large-break LOCA.

It is recommended that the code developers at LANL reexamine the code very carefully for possible coding errors. The constitutive package should be scrutinized again because some of the correlations as used in the code are node-size dependent. Also, various nodalizations, particularly various relative locations of the hot leg penetrations, should be attempted while applying the TRAC-PD2/MOD1 code to the PWR large-break LOCA analyses in order to investigate their effects on the predicted peak clad temperature (PCT).

7. REFERENCES

COLLIER, R. P. (1981), Private Communication, December 10.

CROWLEY, C. J., BLOCK, J. A., and CARY, C. N. (1977), "Downcomer Effects in a 1/15-Scale PWR Geometry - Experimental Data Report," Creare, Inc. NUREG-0281.

CUDNIK, R.A. et al. (1978), Topical Report on Baseline Plenum Filling Behavior in a 2/15-Scale Model of a Four Loop Pressurized Water Reactor, NUREG/CR-0069, BMI-1997

FLANIGAN, L.J. (1982), Private Communication, February 22.

FLANIGAN, L.J. (1983), Private Communication, January 13.

HARPER, R. (1981), "TRAC NEWS", No. 5, Los Alamos National Laboratory,

LILES, D.R. et al. (1981a), TRAC-PD2: An Advanced Best-Estimate Computer Program for Pressurized Water Reactor Loss-of-Coolant Accident Analysis, NUREG/CR-2054, LA-8709-MS.

LILES, D.R. (1981b), Private Communication, June 18.

LILES, D.R. (1983), Letter to F. Odar of USNRC, April 27.

MEIER, J. (1981), Private Communication, July.

SAHA, P. (1981), Letter to F. Odar of USNRC, August 20.

SAHA, P. et al. (1982a), Independent Assessment of TRAC-PD2 and RELAP5/MOD1 Codes at BNL in FY 1981, NUREG/CR-3148, BNL-NUREG-51645.

SAHA, P. (1982b), Letter to D. R. Liles of LANL, October 25.

SCHLICHTING, H. (1968), Boundary-Layer Theory, Sixth Edition, p. 17, McGraw-Hill Book Company, New York.

SEGEV, A., FLANIGAN, L.J., and COLLIER, R.P. (1980), Steam-Water Mixing and System Hydrodynamics Program - Task 4, Quarterly Progress Report, October-December 1979, NUREG/CR-1657, BMI-2062, August.

APPENDIX

TRAC INPUT LISTING FOR TEST ID = 26716

```
              2
ID=BCL26716 RUN.  FRIC=0.235
LOW SUP COOLING POINT
              0
              1                0                19               18
         1.0E-3          1.0E-5          1.0E-4          1.0E-3
             10                0                10                0
              5                4                3                 2                6
              7                8                9                11               15
             10               14               18                19               13
             17                1               12               16E
PIPE                          13               13  BROKEN LEG
              7                0                4                14
              0                1
      5.1054E-2          0.011
              0
        0.90805         0.1397R 5     0.10236E
     7.43565E-3     1.14395E-3R 58.3R1851E-4E
F  8.188596E-3E
           .235R 7          0.0E
F           0.0E
F       0.102108E
F              4E
F            1.0E
F           0.00E
F         403.00E
F         403.00E
F        2.06E05E
BREAK                        17               17  COLD LEG BREAK TO 13
             14                0
         0.10236    8.381851E-4              1.0          372.56     9.956029E4
PIPE                          5                5  STEAM FEED LINE
              1                0               10                5                9
              0                1
      5.0673E-2          0.011
              0
F            0.1E
F       8.067E-4E
F       8.067E-3E
F            0.0E
F            1.0E
F       0.101346E
F              4E
F            1.0E
F           15.0E
F         403.00E
F         403.00E
F      2.6662E05E
PIPE                          4                4  STEAM FEED LINE
              1                0               11                6                9
              0                1
      5.0673E-2          0.011
              0
F            0.1E
F       8.067E-4E
F       8.067E-3E
F            0.0E
F            1.0E
F       0.101346E
F              4E
F            1.0E
F           15.0E
F         403.00E
```

```
F         403.00E
F      2.6662E05E
PIPE                          3              3  STEAM FEED LINE
                1             0             12                7              9
                0             1
       5.0673E-2         0.011
                0
F             0.1E
F       8.067E-4E
F       8.067E-3E
F             0.0E
F             1.0E
F       0.101346E
F                4E
F             1.0E
F            15.0E
F          403.00E
F          403.00E
F      2.6662E05E
PIPE                          2              2  STEAM FEED LINE
                1             0             13                8              9
                0             1
       5.0673E-2         0.011
                0
F             0.1E
F       8.067E-4E
F       8.067E-3E
F             0.0E
F             1.0E
F       0.101346E
F                4E
F             1.0E
F            15.0E
F          403.00E
F          403.00E
F      2.6662E05E
PIPE                         11             11  COLD LEG
                1             0             17                1              9
                0             1
       5.1054E-2         0.011
                0
F             0.1E
F    8.188596E-4E
F    8.188596E-3E
F             0.0E
F             0.0E
F       0.102108E
F                4E
F             0.0E
F            0.00E
F          373.09E
F          373.09E
F      2.6662E05E
PIPE                         10             10  COLD LEG
                1             0             16                2              9
                0             1
       5.1054E-2         0.011
                0
F             0.1E
F    8.188596E-4E
F    8.188596E-3E
F             0.0E
```

```
F           0.0E
F       0.102108E
F              4E
F           0.0E
F          0.00E
F        373.09E
F        373.09E
F     2.6662E05E
PIPE                        18              18 DRAIN
                 1           0              19              18               6
                 0           1
       5.1054E-2         0.011
                 0
F           .05E
F   4.094298E-4E
F   8.188596E-3E
F           0.0E
F           0.0E
F       0.102108E
F              4E
F           1.0E
F          0.00E
F        403.00E
F        403.00E
F     2.6662E05E
FILL                        19              19 DRAIN
              18            7
             .05    4.094298E-4             0.0              .0          403.00
       2.6662E05            .0
VESSEL                       1               1
               9             2               4               9
               9             3               1               0               0
               0
               0
             3.0          10.0            0.01
          7801.0         473.1            43.5             0.6             0.0
             1.0
               0                             1
               0                                             1               1
               0
           .4572          .9144        1.022735        1.201801        1.381252
        1.560703       1.740154        1.943354        2.06375E
          .278003        .309245E
        1.5707963      3.1415927        4.712389       6.2831853E
               8             5               3               1
               8             6               3               2
               8             7               3               4
               8             8               3               3
               9             1               2               5
               9             2               2               6
               9             3               2               7
               9             4               2               8
               1             1              -2              19
F           0.0E
F           0.0E
F           0.0E
F           0.0E
F           0.0E
F           0.0E
F           0.0E
F           0.0E
F           1.0E
F           1.0E
```

```
F          1.0E
R 4        1.0R 4          0.0E
R 4        0.0R 4    0.116975E
R 4        0.0R 4     0.12497E
R 4        0.0R 4          0.0E
R 4        0.0R 4         0.00E
F          1.0E
F          0.0E
F          0.0E
F          0.0E
F          0.0E
F          0.0E
F          0.0E
F        403.00E
F        403.00E
F     2.6662E05E
F          0.0E
F          0.0E
F          0.0E
F          0.0E
F          0.0E
F          0.0E
F          0.0E
F          0.0E
F          1.0E
F          1.0E
F          1.0E
R 4        1.0R 4          0.0E
R 4        0.0R 4     0.12497E
R 4        0.0R 4     0.12497E
R 4        0.0R 4          0.0E
R 4        0.0R 4         0.00E
F          1.0E
F          0.0E
F          0.0E
F          0.0E
F          0.0E
F          0.0E
F          0.0E
F        403.00E
F        403.00E
F     2.6662E05E
F          0.0E
F          0.0E
F          0.0E
F          0.0E
F          0.0E
F          0.0E
F          0.0E
F          0.0E
F          1.0E
F          1.0E
R 4     0.91769R 4          1.0E
R 4        1.0R 4          0.0E
R 4        0.0R 4     0.12497E
R 4        0.0R 4     0.12497E
R 4        0.0R 4          0.0E
R 4        0.0R 4         0.00E
F          1.0E
F          0.0E
F          0.0E
F          0.0E
```

```
F           0.0E
F           0.0E
F           0.0E
F         403.00E
F         403.00E
F     2.6662E05E
F           0.0E
F           0.0E
F           0.0E
F           0.0E
F           0.0E
F           0.0E
F           0.0E
F           0.0E
R 4    0.51769R 4         1.0E
R 4   0.720316R 4         1.0E
R 4    0.51769R 4         1.0E
R 4         0.0R 4         0.0E
R 4         0.0R 4     0.06248E
R 4         0.0R 4     0.06248E
R 4         0.0R 4         0.0E
R 4         0.0R 4        0.00E
F           1.0E
F           0.0E
F           0.0E
F           0.0E
F           0.0E
F           0.0E
F           0.0E
F         403.00E
F         403.00E
F     2.6662E05E
F           0.0E
F           0.0E
F           0.0E
F           0.0E
F           0.0E
F           0.0E
F           0.0E
F           0.0E
R 4    0.51769R 4         1.0E
R 4   0.720316R 4         1.0E
R 4    0.51769R 4         1.0E
R 4         0.0R 4         0.0E
R 4         0.0R 4     0.06248E
R 4         0.0R 4     0.06248E
R 4         0.0R 4         0.0E
R 4         0.0R 4        0.00E
F           1.0E
F           0.0E
F           0.0E
F           0.0E
F           0.0E
F           0.0E
F           0.0E
F         403.00E
F         403.00E
F     2.6662E05E
F           0.0E
F           0.0E
F           0.0E
F           0.0E
F           0.0E
F           0.0E
F           0.0E
F           0.0E
```

```
R 4     0.51769R 4          1.0E
R 4    0.720316R 4          1.0E
R 4     0.51769R 4          1.0E
R 4          0.0R 4          0.0E
R 4          0.0R 4      0.06248E
R 4          0.0R 4      0.06248E
R 4          0.0R 4          0.0E
R 4          0.0R 4         0.00E
F            1.0E
F            0.0E
F            0.0E
F            0.0E
F            0.0E
F            0.0E
F            0.0E
F          403.00E
F          403.00E
F       2.6662E05E
F            0.0E
F            0.0E
F            0.0E
F            0.0E
F            0.0E
F            0.0E
F            0.0E
F            0.0E
R 4     0.51769R 4          1.0E
R 4    0.720316R 4          1.0E
R 4     0.51769R 4          1.0E
R 4          0.0R 4          0.0E
R 4          0.0R 4      0.06248E
R 4          0.0R 4      0.06248E
R 4          0.0R 4          0.0E
R 4          0.0R 4         0.00E
F            1.0E
F            0.0E
F            0.0E
F            0.0E
F            0.0E
F            0.0E
F            0.0E
F          403.00E
F          403.00E
F       2.6662E05E
F            0.0E
F            0.0E
R 4          0.0    0.012748686      1.2621199    0.012748686      1.2621199E
R 4          0.0    0.012748686      1.2621199    0.012748686      1.2621199E
F            0.0E
F            0.0E
F            0.0E
F            0.0E
R 4     0.51769          0.9904          0.6773         0.9904          0.6773E
R 4    0.720316             1.0            0.51            1.0            0.51E
R 4     0.51769R 4          1.0E
R 4          0.0R 4          0.0E
R 4          0.0         0.05766         0.0596         0.05766         0.0596E
R 4          0.0          0.0604          0.0591          0.0604          0.0591E
R 4          0.0R 4          0.0E
R 4          0.0R 4         0.00E
F            1.0E
F            0.0E
```

```
F           0.0E
F           0.0E
F           0.0E
F           0.0E
F           0.0E
F         403.00E
F         403.00E
F      2.6662E05E
F           0.0E
F           0.0E
F           0.0E
F           0.0E
F           0.0E
F           0.0E
F           0.0E
F           0.0E
R 4     0.51769R 4          1.0E
R 4     0.72031GR 4         1.0E
F           0.0E
R 4         0.0R 4          0.0E
R 4         0.0R 4      0.05531E
F           0.0E
R 4         0.0R 4          0.0E
R 4         0.0R 4         0.00E
F           1.0E
F           0.0E
F           0.0E
F           0.0E
F           0.0E
F           0.0E
F           0.0E
F         403.00E
F         403.00E
F      2.6662E05E
PIPE                       12              12  COLD LEG
                1                          0  15                  3                   9
                0                          1
       5.1054E-2                   0.011
                0
F           0.1E
F   8.188596E-4E
F   8.188596E-3E
F           0.0E
F           0.0E
F       0.102108E
F             4E
F           0.0E
F          0.00E
F         373.09E
F         373.09E
F      2.6662E05E
FILL                       15              15  COLD LEG FILL TO 11
               17                          7   0                   0
              0.1     8.188596E-4           0.0             .000            373.09
       2.6662E05        7.679319
FILL                       14              14  COLD LEG FILL TO 10
               16                          7   0                   0
              0.1     8.188596E-4           0.0             .000            373.09
       2.6662E05        7.679319
FILL                       16              16  COLD LEG FILL TO 12
               15                          7   0                   0
              0.1     8.188596E-4           0.0             .000            373.09
       2.6662E05        7.679319
```

```
FILL                                6         6  STEAM FEED TO 5
           10                       7
          0.1               8.067E-4        1.0          00.0          403.0
  2.6662025E5               .3001648
FILL                                7         7  STEAM FEED TO 4
           11                       7
          0.1               8.067E-4        1.0          00.0          403.0
  2.6662025E5               .3001648
FILL                                8         8  STEAM FEED TO 3
           12                       7
          0.1               8.067E-4        1.0          00.0          403.0
  2.6662025E5               .3001648
FILL                                9         9  STEAM FEED TO 2
           13                       7
          0.1               8.067E-4        1.0          00.0          403.0
  2.6662025E5               .3001648
       1.0E-8                   0.01       32.0        1000.0
         0.25                   0.25       0.50          0.25
-1.00000
```

DISTRIBUTION

USNRC

O. E. Bassett
W. D. Beckner
Y. S. Chen
C. Graves, NRR
J. Guttmann, NRR
M. W. Hodges, NRR
C. N. Kelber
R. Lee
R. B. Minogue
W. Morrison
F. Odar
J. N. Reyes
D. F. Ross
B. Sheron, NRR
L. M. Shotkin
H. S. Tovmassian
M. Young
N. Zuber

BNL

H. J. C. Kouts
W. Y. Kato
DNE Associate Chairmen
NSP Division Heads and
Group Leaders
LWR CAAG Staff
Nuclear Safety Library (2)

External

D. R. Liles, LANL
T. D. Knight, LANL

T. R. Charlton, INEL

D. Majumdar, DOE/Idaho

L. D. Buxton, SNL

R. P. Collier, BCL
L. J. Flanigan, BCL

I. Brittain, Winfrith (U.K.)
J. Fell, Winfrith (U.K.)

NRC FORM 335 (11 81)

U.S. NUCLEAR REGULATORY COMMISSION

BIBLIOGRAPHIC DATA SHEET

1. REPORT NUMBER (Assigned by DDC)
NUREG/CR-4252
BNL-NUREG-51886

4. TITLE AND SUBTITLE (Add Volume No., if appropriate)
Independent Assessment of TRAC-PD2/MOD1 Code with BCL ECC Bypass Tests

2. (Leave blank)

3. RECIPIENT'S ACCESSION NO.

7. AUTHOR(S)
G. C. Slovik and P. Saha

5. DATE REPORT COMPLETED
MONTH: March | YEAR:

DATE REPORT ISSUED
MONTH | YEAR

9. PERFORMING ORGANIZATION NAME AND MAILING ADDRESS (Include Zip Code)
Department of Nuclear Energy
Brookhaven National Laboratory
Upton, Long Island, New York 11973

6. (Leave blank)

8. (Leave blank)

12. SPONSORING ORGANIZATION NAME AND MAILING ADDRESS (Include Zip Code)
Division of Accident Evaluation
Office of Nuclear Regulatory Research
U.S. Nuclear Regulatory Commission
Washington, DC 20555

10. PROJECT/TASK/WORK UNIT NO.

11. FIN NO.
A-3257

13. TYPE OF REPORT
Technical Report

PERIOD COVERED (Inclusive dates)

15. SUPPLEMENTARY NOTES

14. (Leave blank)

16. ABSTRACT (200 words or less)

This report presents the TRAC-PD2/MOD1 independent assessment calculations performed at Brookhaven National Laboratory (BNL) using the Emergency Core Cooling (ECC) bypass experiments conducted in a 2/15-scale PWR vessel at Battelle Columbus Laboratories (BCL). Both steady-state experiments with various ECC water subcoolings and transient tests with hot wall effects were simulated. Besides the base cases, several sensitivity calculations were performed to study the effects of nodalization, particularly the relative locations of the hot leg penetrations in the downcomer. In addition, calculations were performed to determine the effect of slight increases in the reverse core steam flow and the associated form losses due to the hot leg penetrations. Code corrections as recenved from the code developers at Los Alamos National Laboratory (LANL) were also incorporated into this study.

17. KEY WORDS AND DOCUMENT ANALYSIS

17a. DESCRIPTORS

TRAC-PD2/MOD1
Emergency Core Cooling (ECC)
Bypass Tests
PWR

17b. IDENTIFIERS/OPEN-ENDED TERMS

18. AVAILABILITY STATEMENT
Unliminted

19. SECURITY CLASS (This report)
Unclassified

21. NO. OF PAGES

20. SECURITY CLASS (This page)

22. PRICE

NRC FORM 335 (11 81)